Coordination of NNN iminophosphorane ligands to MnII, CoII, and FeII and application in the transfer hydrogenation of ketones

Ingrid Popovici, Thibault Tannoux, Sophie Bourcier, Nicolas Casaretto, Audrey Auffrant

Coordination of NNN iminophosphorane ligands to Mn^{II}, Co^{II}, and Fe^{II} and application in the transfer hydrogenation of ketones

Ingrid Popovici, Thibault Tannoux, Sophie Bourcier, Nicolas Casaretto, and Audrey Auffrant*

Laboratoire de Chimie Moléculaire (LCM), CNRS, Ecole polytechnique, Institut Polytechnique de Paris, Route de Saclay, 91120 Palaiseau, France.

E-mail: audrey.auffrant@polytechnique.edu

Keywords: Manganese, cobalt, Iminophosphorane, NNN ligands, transfer hydrogenation catalysis

Highlights:

- Synthesis of an original NNN ligand with three different N coordinating groups
- Synthesis and characterization of NNN Fe^{II}, Co^{II}, Mn^{II} complexes
- Transfer hydrogenation catalysis of ketones with earth abundant metal complexes
- First report of iminophosphorane Mn^{II} catalyst

Abstract: Tridentate NNN ligands combining three different N-coordinating groups; a pyridine, a secondary amine, and an iminophosphorane were synthesized ($\mathbf{L^R}$, R= Et, Cy, Ph). They were coordinated to Fe^{II}, Co^{II}, and Mn^{II} to yield high spin complexes as indicated by the magnetic moment measured in solution. They were also characterized by ^{1}H NMR spectroscopy, HR-MS, elemental analysis, as well as X-ray diffraction for some of them. Depending on the nature of the P-substituent, ligand exchange occurs in solution leading to octahedral complexes featuring two $\mathbf{L^{Cy}}$ ligand coordinated in a κ^2 mode. The latter were also independently prepared. All the synthesized complexes were compared in the catalytic transfer hydrogenation of ketones. $\mathbf{L^{Et}}$ supported complexes performed better and the reaction was optimized for the Co^{II} and Mn^{II} complexes because these metals are more rarely employed for this reaction than Fe^{II}. Both complexes proved able to efficiently reduce a range of aromatic and aliphatic ketones within 24 h at 70°C using 1 mol% catalyst in presence of 20 mol % of ^{t}BuOK. The reaction is facilitated by the presence of electron-withdrawing and the absence of coordinating atom in the substrate. Moreover, for aliphatic ketones, while acyclic derivatives and linear methylketones convert very efficiently, substrates with long linear alkyl chain did not react. Regarding the mechanism, some additional experiments allow to suggest, despite the paramagnetic nature of the precatalysts, the involvement of M-H species.

1. Introduction

Transition-metal catalyzed transfer hydrogenation (TH) reactions have appeared as a valuable alternative to hydrogenations for achieving the reduction of polar bonds. Indeed, while the direct hydrogenation requires the use of pressurized H_2 that may be hazardous and/or require specific experimental setups, in TH reactions easy-to-handle and abundant hydrogen donor molecules are employed.[1]

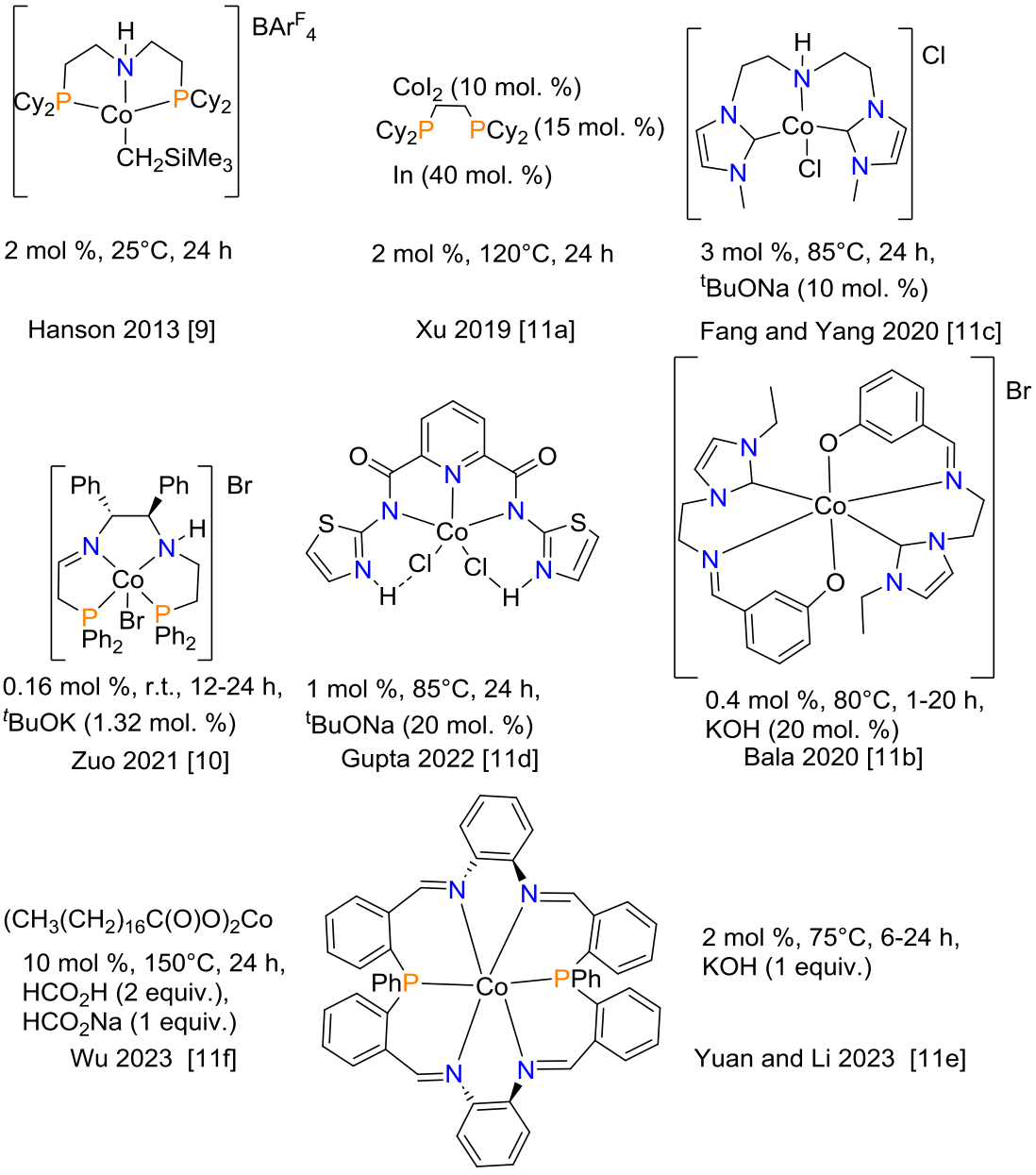

Chart 1: Previous transfer hydrogenation catalysts

The field was dominated in the past years by noble metals[2] Ir, Rh, and in particular Ru based catalysts, but for about two decades alternative catalytic systems involving abundant metals have emerged.[3] Because its position in the periodic table, iron(II) has attracted a lot of attention. Fe^0 and Fe^{II} in association with N_3 and N_4 ligands (terpyridine, bis(pyrazolyl)pyridine, and porphyrin), phosphine-amine or -imine Fe^{II} complexes, as well as Knölker-type or NHC supported iron carbonyl

complexes were shown to efficiently catalyze this reaction.[4] Catalysts involving other earth-abundant metal like Ni, Co, Mn are much less represented.[5] Some Ni^0 and Ni^{II} catalysts were described.[6] Regarding Mn, most ketone transfer hydrogenations have been catalyzed by Mn^I carbonyl complexes,[7] while only one Mn^{II} catalyst, a macrocyclic carboxamide dimer was recently reported.[8] For cobalt eight different catalysts whose structures are shown in Chart 1 with a summary of their catalytic performances are known. The best catalyst was the one described by Hanson in 2013 which is able to transform both aromatic and aliphatic ketones at room temperature within 24 h.[9] The other catalyst operating at room temperature is the N_2P_2 Co^{II} complex reported by Zuo. It works at very low catalyst loading but proved more sensitive to substituent effects.[10] The other Co catalysts proceed within 1 to 24 h at temperatures between 75°C and 150°C.[11] Interestingly most of these catalysts incorporate N-donor groups and/or strong σ-donating moiety (NHC, alkylphosphine, amide). Given our interest for iminophosphorane ligands which are strong electron N-based donor groups,[12] we wondered if they would be able to lead to efficient base metal catalysts for the transfer hydrogenation of ketones.

1) Previous transfer hydrogenation catalysts featuring iminophosphorane ligands

V. Cadierno, J. Gimeno, & M. A. Rodriguez [13]

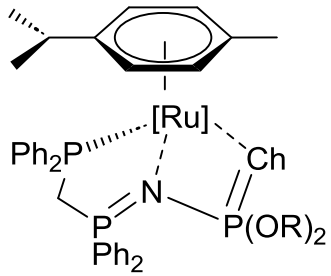

Ch= S, O

[Ru]= $RuCl_2$ (κ^1-P),
$RuCl^+$(κ^2-P,N/Ch)
Ru_2^+(κ^3-P,N, Ch)

S. Sabo-Etienne, P. Le Floch, A. Auffrant [14,15]

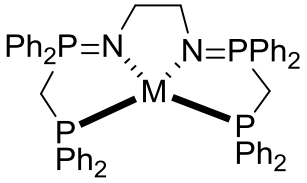

M= RuH^+, RuHCl, $RhCl_2^+$

P. Le Floch, A. Auffrant [16]

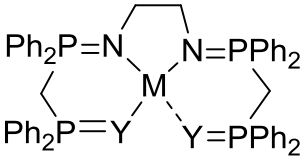

Y= lone pair, S, O

M =$FeCl_2$, $FeCl^+$, $Fe(CNMe)_2^{2+}$

2) This work

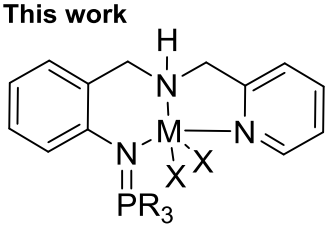

MX_2= $FeCl_2$, $CoCl_2$, $MnBr_2$
R= Et, Cy, Ph

Chart 2: Previous related iminophosphorane catalysts and targeted complexes

Even if the catalytic applications of iminophosphorane ligands are much less developed than those of their carbene or imine counterparts, catalysts involving noble metals were described for this transformation (Chart 2). Cadierno reported about 20 years ago, Ru^{II} catalysts supported by PNO/S ligands[13] and our team described Ru^{II} complexes featuring NNP and P_2N_2 ligands[14] as well as P_2N_2 Rh^{III} complexes.[15] We are only aware of one report involving iminophosphorane earth-abundant metal complexes namely P_2Y_2 (Y=N, S, O) Fe^{II} complexes.[16] With this in mind, we designed for this project a tridentate L_3 ligand associating three different nitrogen donors: a pyridine, a secondary amine and an iminophosphorane. This is a rather original ligand structure since the only comparable example we could find is the heteroscorpionate bispyrazolyliminophosphorane synthesized by Cui,

Zhang and coworkers which was used to prepare lanthanide, calcium, and zinc catalysts.[17] In this paper, we report the synthesis of three tridentate NNN monoiminophosphorane ligands, their coordination to Fe^{II}, Co^{II}, and Mn^{II} (Chart 2) as well as the use of these complexes to catalyze the transfer hydrogenation of ketones.

2. Results and Discussion

2.1 Ligand synthesis and coordination study

The synthesis of the targeted NNN ligand associating an iminophosphorane, a pyridine, and an amine was realized via a nucleophilic substitution by the picolylamine of the halide in 1-Azido-(2-halogenomethyl)benzene (Scheme 1). The reaction was initially conducted in stoichiometric proportions and led to an ammonium resulting from a double substitution (Scheme S1). The structure of the formed product was ascertained by X-ray diffraction (Figure S71). In order to obtain the targeted ligand precursor featuring a central secondary amine group, the reaction was conducted with an excess of picolylamine which served both as a nucleophile and a base. An optimization regarding the reaction temperature, solvent, and duration as well as the nature of the halide (Br or Cl) was conducted (see Table S1). The best results were obtained in CH_2Cl_2 at room temperature using 10 equivalents of picolylamine and 1-Azido-(2-bromomethyl)benzene leading to the secondary amine **1** in 84% yield. It was characterized by ^{1}H, ^{13}C NMR spectroscopy, and HR-MS.

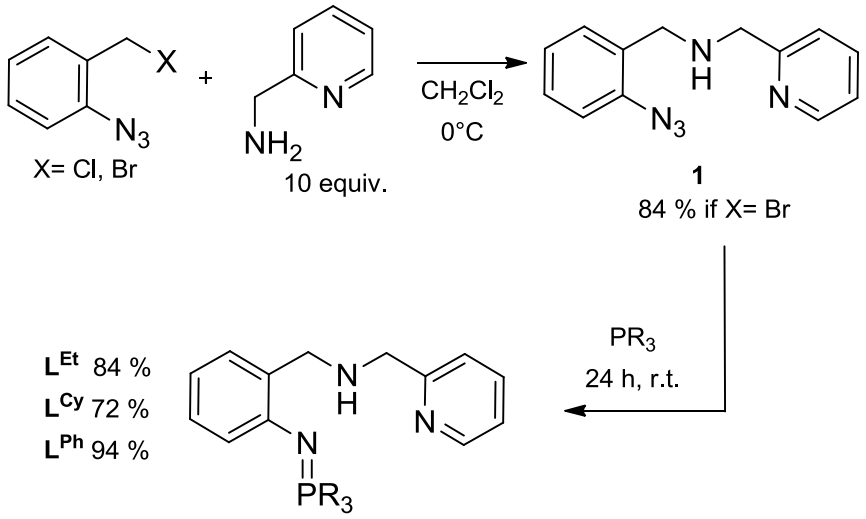

Scheme 1: Synthesis of NNN ligand L^R

The iminophosphorane was then generated by a Staudinger reaction with a phosphine; triethyl-, tricyclohexyl-, and triphenyl-phosphine were employed allowing the isolation of ligand $\mathbf{L^{Et}}$, $\mathbf{L^{Cy}}$, and $\mathbf{L^{Ph}}$ in respectively 84, 72, 94% (Scheme 1). No reaction was observed with sterically hindered tris(mesityl)phosphine even upon forcing conditions. Of note, $\mathbf{L^R}$ exhibits three nitrogen-based neutral coordination sites of different natures. The ^{31}P resonance[18] changes with the nature of the substituent on P, it was observed at 22.8 and 20.5 ppm for $\mathbf{L^{Et}}$, and $\mathbf{L^{Cy}}$ respectively while the resonance of $\mathbf{L^{Ph}}$ appears at 0.1 ppm, which all are in the range of reported data for similar iminophosphoranes.[19] The ^{1}H and ^{13}C NMR spectra mostly differ by the resonances due to the P-substituents, but there is a large deshielding (almost 1 ppm) of the NH resonance in $\mathbf{L^{Et}}$ or $\mathbf{L^{Cy}}$ (δ= 3.43 and 3.47 ppm respectively) compared to $\mathbf{L^{Ph}}$ (δ= 2.48 ppm). This may be ascribed to an intramolecular

H-bond between the iminophosphorane N atom and the proton of the amine, the latter being stronger with the more basic alkyl-substituted iminophosphorane. Single crystals of $\mathbf{L^{Ph}}$ were grown by diffusion of Et_2O in saturated THF solutions (Figure 1). Compared to the 2-iminophosphoranylbenzamide previously described,[20] the P=N is shorter (1.5674(11) vs 1.601(8) Å) and the N···H-NH weaker (2.425 Å vs 2.023 Å). nevertheless, the measured distance being smaller than the sum of the van der Waals radii, a weak interaction is present in the solid state. It is probably maintained in solution based on the NH chemical shift differences observed by ^{1}H NMR.

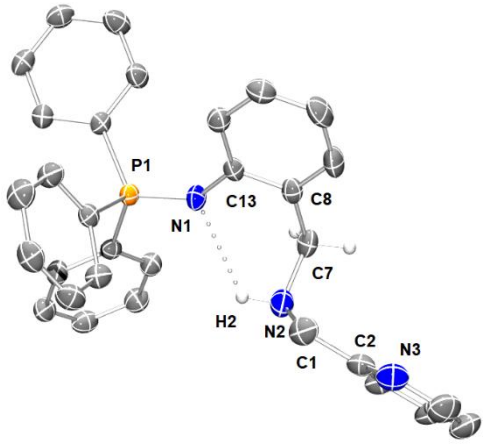

Figure 1: X-ray structure of $\mathbf{L^{Ph}}$. Most H atoms, a CH_2Cl_2 and a water molecule were omitted for clarity. Selected bond lengths [Å] and angles [°]:P1-N1 = 1.5674(11); N1-C1 = 1.507(4); N1-C13 = 1.3901(6); C7-N2: 1.4740(17); N2-C1: 1.4506(19); C13−N1−P1 = 129.67(9); N2-C7−C8 = 115.65(10); C13−C8−C7 = 129.00(12); C1-N2-C7: 113.38(12); N2-C1-C2 = 113.47(11).

Given our interest in the reactivity of earth-abundant metal complexes, we investigated the coordination of these ligands to Fe^{II}, Co^{II}, and Mn^{II} centers (Scheme 2). Complexes were formed by stirring the ligand $\mathbf{L^R}$ with a stoichiometric amount of $FeCl_2$, $CoCl_2$, or $MnBr_2$ overnight at room temperature. In all cases, the coordination induced the loss of the ^{31}P resonance due to the formation of a paramagnetic complex. Complexes $\mathbf{[Fe(L^R)Cl_2]}$ were isolated as green solids in respectively 42, 52, and 69% yield (R= Et, Cy, Ph)**.** $\mathbf{[Co(L^R)Cl_2]}$ were isolated as blue or purple solids in 62-77% yield. The Mn^{II} complexes were isolated after removal of the solvent and washing with pentane as light-yellow solids in high yield. Such Mn^{II} complexes supported by a mixed iminophosphorane polydentate ligand are rare in the literature, we are only aware of two Mn^{II} bis(iminophosphoranyl)methanide ligands reported by Hill and coworkers twenty years ago.[21]

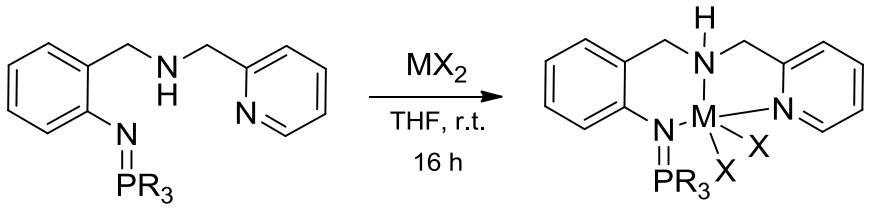

$[Fe(L^R)Cl_2]$

R = Et (42%), Cy (52%), Ph (69%)

$[Co(L^R)Cl_2]$

R = Et (77%), Cy (62%), Ph (72%)

$[Mn(L^R)Br_2]$

R = Et (80%), Cy (74%), Ph (77%)

Scheme 2: Synthesis of $\mathbf{L^R}$ supported complexes

Because of the paramagnetism of these complexes their ^{1}H NMR spectrum shows broad resonances across a large chemical shift window that are poorly informative (Figures S11-19). Nevertheless, the spectrum is different for each complex and this allowed confirming the reproducibility of the coordination reactions by comparison between experiences. These complexes were also characterized by HR-Ms and elemental analysis. Their magnetic moment was measured in solution following the Evans methodology.[22] The measured values are consistent with high spin d^6 (**[Fe($\mathbf{L^R}$)$\mathbf{Cl_2}$]**, 5.22, 4.92, and 4.94 μ_B, S=2), d^7 (**[Co($\mathbf{L^R}$)$\mathbf{Cl_2}$]**, 4.32, 4.22, and 4.31 μ_B, S=3/2), and d^5 (**[Mn($\mathbf{L^R}$)$\mathbf{Br_2}$]**, 6.05, 6.37, and 5.99 μ_B, S=5/2) corresponding to an electronic configuration with respectively four, three, and five unpaired electrons. Surprisingly, while single crystals formed quite rapidly for $\mathbf{L^{Et}}$ supported Fe^{II}, Co^{II}, and Mn^{II} complexes (**[M($\mathbf{L^{Et}}$)$\mathbf{X_2}$]**), for the other complexes, crystallization generally failed or took months whichever the metal (vide infra). Only **[Mn($\mathbf{L^{Cy}}$)$\mathbf{Br_2}$]** formed suitable crystals after multiple attempts The X-ray structures of complex **[M($\mathbf{L^{Et}}$)$\mathbf{X_2}$]** and **[Mn($\mathbf{L^{Cy}}$)$\mathbf{Br_2}$]** are shown in Figure 2**.** Note that for **[Mn($\mathbf{L^{Et}}$)$\mathbf{Br_2}$]** the lattice contains three rather similar molecules only one is presented in Figure 2, the others in Figure S72. For **[Mn($\mathbf{L^{Cy}}$)$\mathbf{Br_2}$]** two similar molecules were observed, the second one is presented in Figure S73.

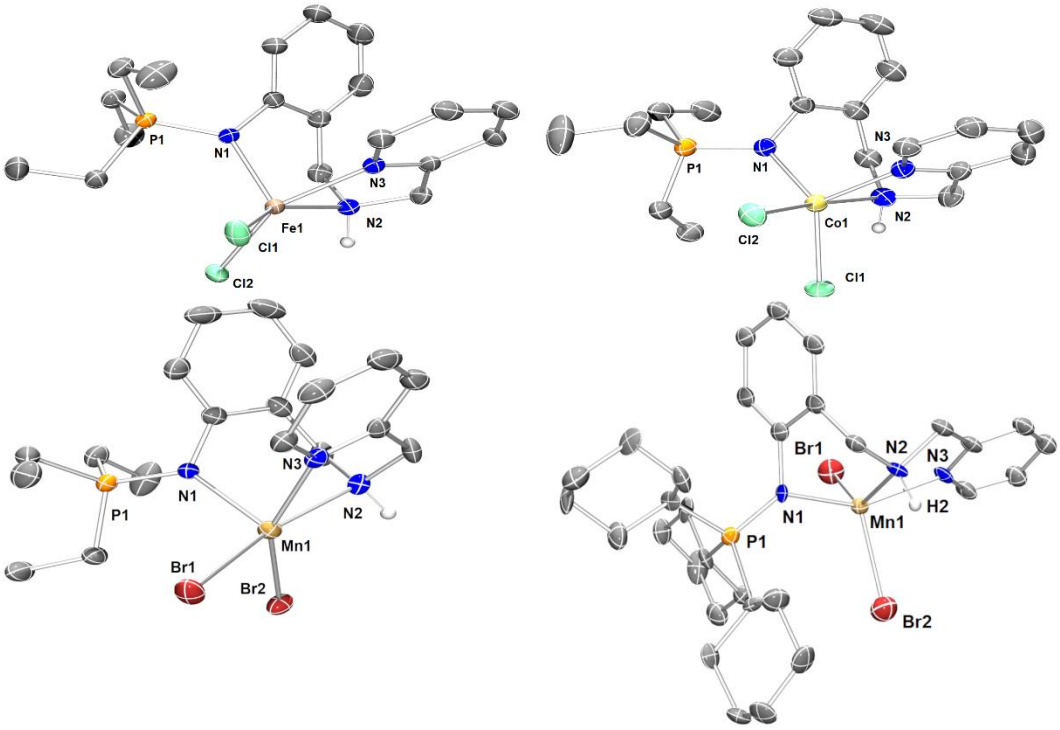

Figure 2: X-structures of **[Fe($\mathbf{L^{Et}}$)$\mathbf{Cl_2}$]** (top left), **[Co($\mathbf{L^{Et}}$)$\mathbf{Cl_2}$]** (top right), and **[Mn($\mathbf{L^{Et}}$)$\mathbf{Br_2}$]** (bottom) with thermal ellipsoids (drawn at the 50% probability level). Most H atoms and solvent molecules were omitted for clarity. Selected bond lengths (Å) and angles (°): **[Fe($\mathbf{L^{Et}}$)$\mathbf{Cl_2}$]** Fe1-Cl1 2.3465(5), Fe1-Cl2 2.3935(5), Fe1-N1 2.1031(13), Fe1-N2 2.2048(14), Fe1-N3 2.2198(14), P1-N1 1.6248(14), N1-Fe1-N3 93.47(5), N1-Fe1-N2 92.03(5), N2-Fe1-N3 75.18(5), N3-Fe1-Cl2 153.01(4), N2-Fe1-Cl1 151.90(4); **[Co($\mathbf{L^{Et}}$)$\mathbf{Cl_2}$]** Co1-Cl1 2.3109(8), Co1-Cl2 2.3781(8), Co1-N1 2.024(2), Co1-N2 2.228(2), Co1-N3 2.072(2), P1-N1 1.613(3), N1-Co1-N3 105.77(10), N1-Co1-N2 85.85(10), N3-Co1-N2 77.87(9), N3-Co1-Cl2 95.74(7), N2-Co1-Cl1 84.79(7); **[Mn($\mathbf{L^{Et}}$)$\mathbf{Br_2}$]** Mn1-Br1 2.5765(7), Mn1-Br2 2.6114(7), Mn1-N1 2.219(3), Mn1-N2 2.281(3), Mn1-N3 2.248(3), P1-N1 1.611(14), N1-Mn1-N3 91.31(10), N1-Mn1-N2 87.07(10), N2-Mn1-N3 74.23(11), N3-Mn-Br1 97.54, N2-Mn1-Br1 164.94(4), Br1-Mn1-Br2 98.79(2). **[Mn($\mathbf{L^{Cy}}$)$\mathbf{Br_2}$]** Mn1-Br1 2.5548(19), Mn1-Br2 2.499(2), Mn1-N1 2.207(8), Mn1-N2 2.311(8), Mn1-N3

2.275(9), P1-N1 1.603(9), N1-Mn1-N3 148.7(3), N1-Mn1-N2 83.4(3), N3-Mn1-N2 71.9(3), N3-Mn1-Br1 89.8(2), N2-Mn1-Br1 139.4(2), Br2-Mn1-Br1112.50(7).

In **[Fe(L^{Et})Cl_2]** the iron is pentacoordinated and presents a distorted square based pyramidal geometry (τ_5[23]=0.02), where the iminophosphorane N1 atom is in apical position. In this complex, the three N-based coordinating groups are of different nature, and the shortest Fe-N bond is observed with the iminophosphorane and the longest one with the pyridine. In the cobalt analogue **[Co(L^{Et})Cl_2]**, a trigonal bipyramid geometry (τ_5=0.85) is observed in which the NH and one chloride occupy the apical positions. The Co-N bond lengths increase as in **[Fe(L^{Et})Cl_2]** from M-N=P, to M-NH, and M-N_{pyr}. Moreover, in agreement with the shorter ionic radius of Co^{2+} compared to Fe^{2+}, the bond lengths (M-Cl and M-N) measured in **[Co(L^{Et})Cl_2]** are shorter than the corresponding ones in **[Fe(L^{Et})Cl_2]**. For the Mn^{II} complex the observed geometry depends on the ligand. **[Mn(L^{Et})Br_2]** is square based pyramidal (τ_5=0.15) as in **[Fe(L^{Et})Cl_2]** with the N1 iminophosphorane atom also in apical position. In **[Mn(L^{Cy})Br_2]** a trigonal bipyramid geometry is observed (τ_5=0.61) with N1 and N3 forming the vertical axis . Because of the largest ionic radius of Mn^{II} compared to Fe^{II}, and Co^{II}, in both cases, the Mn-N bonds are longer than the Fe-N and Co-N ones. Moreover, they increase from M-N=P, M-N_{pyr}, to M-NH, which differs from the evolution observed in the Fe and Co complexes. The nature of the ligand does not impact much the Mn—N bonds, but because of the difference of geometry there is a difference in the Br-Mn-Br angles and the Mn-Br bond lengths. The former is wider and the latter

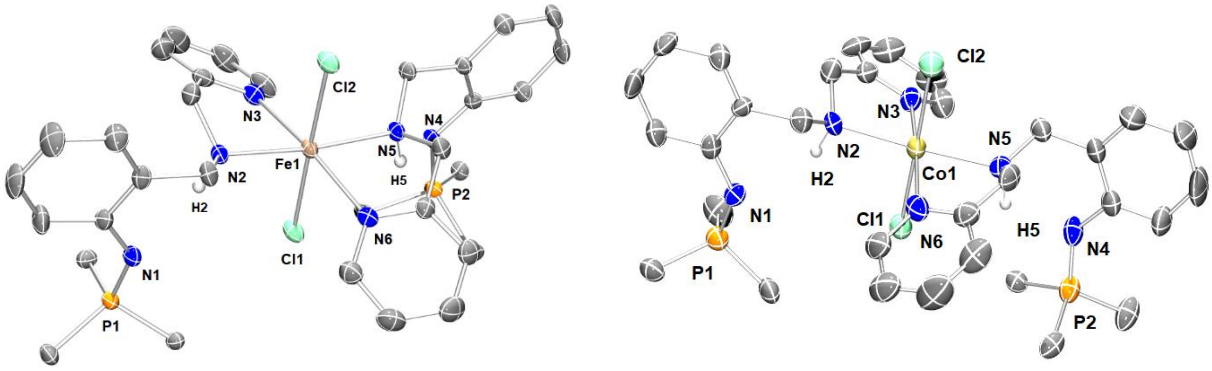

are shorter with **L^{Cy}**. Of note the N=P bond lengths are very similar in these four complexes.

Figure 3: X-structures of **[Fe(L^{Cy})$_2$$Cl_2$]** (left) and **[Co($L^{Cy}$)$_2$$Cl_2$]** (right) with thermal ellipsoids (drawn at the 50% probability level). Most H atoms, all the methylene carbons of the Cy substituents and two CH_2Cl_2 molecules (for **[Fe(L^{Cy})$_2$$Cl_2$]**) were omitted for clarity. Selected bond lengths (Å) and angles (°): **5^{Cy}** Fe1-Cl2 2.4337(9), Fe1-Cl1 2.4384(9), Fe1-N2 2.227(3), Fe1-N3 2.242(3), Fe1-N5 2.227(3), Fe1-N6 2.235(3), P1-N1 1.590(3), P2-N4 1.583(3), N2-Fe1-N3 75.93(10), N5-Fe1-N3 107.89(10), N5-Fe1-N6 74.55(10), N2-Fe1-N6 102.61(10)), N6-Fe1-N3 170.10(11), Cl2-Fe1-Cl1 178.80(4); **6^{Cy}** Co1-Cl2 2.435(2), Co1-Cl1 2.426(2), Co1-N2 2.179(5), Co1-N3 2.193(6), Co1-N5 2.192(5), Co1-N6 2.171(6), P1-N1 1.564(6), P2-N4 1.578(7), N2- Co1-N3 76.6(2), N5-Co1-N3 105.6(2), N6-Co1-N5 76.5(2), N2-Co1-N6 102.1(2), N6-Co1-N3 170.9(3), Cl2- Co1-Cl1 178.88(4).

As stated previously, except for **[Mn(L^{Cy})Br_2]**, no X-ray structure could be obtained for **[M(L^{R})X_2]** (R= Cy, Ph), but single crystals formed after long standing (a few months) from dichloromethane solutions of **[Fe(L^{Cy})Cl_2]** and **[Co(L^{Cy})Cl_2]**. The corresponding X-ray structures are given in Figure 3, they show the formation of **[M(L^{Cy})$_2$$Cl_2$]** (with M= Fe, Co) complexes probably resulting from a ligand scrambling process. In these structures, the metal is coordinated by the secondary amine and the pyridine of the two ligands while the iminophosphorane remain uncoordinated. Interestingly, with a PNN ligand the preferential coordination of iminophosphorane to Fe^{II} over the phosphine was

observed.[24] **[M(L^{Cy})$_2$Cl$_2$]** (M =Fe, Co) exhibit a distorted octahedral geometry; with N3N5N6N2 torsion angle measures -9.66° and -8.76° for M=Fe and Co respectively. The bond lengths and angles are very similar within the two structures, the Fe coordination bonds are slightly longer because of the difference in ionic radius between Fe^{2+} and Co^{2+}. The uncoordinated iminophosphorane bonds (1.583(3) and 1.590(3) Å in **[Fe(L^{Cy})$_2$Cl$_2$]** and 1.564(6) and 1.578(7) Å in **[Co(L^{Cy})$_2$Cl$_2$]**) are comparable to that reported for free 2,6-(tricyclohexylphosphinoiminemethyl)pyridine but shorter than coordinated ones[19] which agrees well with an increased negative hyperconjugation between N and P in free iminophosphoranes. Of note, in both structures short contacts exist between the H of the secondary amines (H_2 and H_5) and the N of the iminophosphorane (respectively N_1 and N_4).

To verify that **[M(L^{Cy})$_2$Cl$_2$]** formed from **[M(L^{Cy})Cl$_2$]** (M= Fe, Co), these complexes were directly prepared by reacting two equivalents of **L^{Cy}** with $FeCl_2$ and $CoCl_2$ respectively (Scheme 3). In each case, the ^{1}H NMR spectrum of the formed product was rather different from the one obtained in the stoichiometric reaction (Figures S12, 15, 20, 21) but similar to the one obtained from the crystals formed after long standing solutions of **[M(L^{Cy})Cl$_2$]** (M= Fe, Co). In addition, complexes formed in the 2 : 1 reaction crystallized rapidly (within a few hours) and the corresponding X-ray structures were identical to those obtained after letting stand **[M(L^{Cy})Cl$_2$]** solutions for months in the glovebox. Therefore, we concluded that **[M(L^{Cy})$_2$Cl$_2$]** (M= Fe, Co) evolved in solution through ligand scrambling. The same reaction failed from $MnBr_2$ because the **[M(L^{Cy})Br$_2$]** precipitated out of the reaction medium, leaving one equivalent of unreacted ligand in the supernatant. As **L^{Cy}** is not soluble in toluene, THF or acetonitrile and decomposes rapidly in chlorinated solvents it was not possible to attempt this reaction in another solvent.

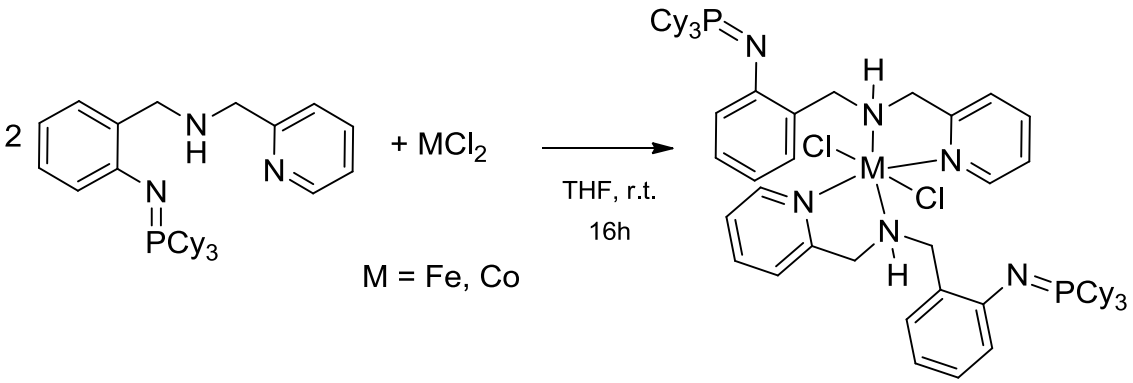

Scheme 3: Direct Synthesis of **[M(L^{Cy})$_2$Cl$_2$]** (M= Fe, Co).

The process was monitored by ^{1}H NMR spectroscopy. As it lasts several weeks, it was accelerated by heating solutions of **[M(L^{Cy})X$_2$]** (M= Fe, Co, Mn; X= Cl, Br) in $CDCl_3$ at 70°C for several days (Figure S68, 69). The ^{1}H NMR monitoring of the crude mixture showed the slow formation of the 2:1 complex. This was accompanied by a color change from green to brown for iron, from blue to green for cobalt, and from white to yellow for manganese. After 2 or 4 days for Fe and Co respectively, the ^{1}H NMR spectrum obtained matched that of the **[M(L^{Cy})$_2$Cl$_2$]** complex (M= Fe, Co). For manganese, the disappearance of a broad singlet at 3.93 ppm characteristic of the **[Mn(L^{Cy})Br$_2$]** complex was observed after 7 days (Figure S70). Nevertheless, no crystal could be formed to ascertain the formation of **[Mn(L^{Cy})$_2$Br$_2$]**.

No further information could be obtained for **[M(L^{Ph})X_2]** (M= Fe, Co, Mn, X= Cl, Br) since no single crystals could be grown for these complexes, despite several attempts.

2.2 Catalytic transfer hydrogenation of ketones

The performances of **[M(L^{R})Cl_2]** and **[M(L^{Cy})$_2Cl_2$]** complexes were compared for the transfer hydrogenation of ketones (Table 1). This reaction was catalyzed by different mixed iminophosphorane ligand supported Ru^{II}[13-14] and one Rh^{III}[15] complexes, but examples of iminophosphorane containing earth abundant metal complexes remain limited to Fe^{II} complexes supported by iminophosphorane N_2Y_2 ligand (Y= P, O, S).[16] We first chose to compare the three **L^{Et}** supported complexes for the transfer hydrogenation of acetophenone. The reaction was conducted in pure isopropanol at 70°C using 1 mol. % catalyst in presence of 20% of ^{t}BuOK as a base. After 6 h, only the **[Fe(L^{Et})Cl_2]** led to a moderate yield (Entries 1-3). Nevertheless, these performances were lower than those reported with N_2Y_2 Fe^{II} complexes, which exhibit better performances with only 0.1 mol. % catalyst.[16] Therefore, we decided to focus on Co^{II} and Mn^{II} complexes because these metals were much less employed in transfer hydrogenation catalysis than iron, and almost never used in combination with iminophosphorane ligands for catalyst development.

Good to average yields were obtained by extending the reaction time to one day (entries 4 and 5). Then, a higher concentration was employed (2 M) leading to excellent NMR yields with both **[Co(L^{Et})Cl_2]** and **[Mn(L^{Et})Br_2]** (entries 6-7). Note that complete conversion was observed after respectively 28h and 26h for **[Co(L^{Et})Cl_2]** and **[Mn(L^{Et})Br_2]**, pointing towards a lower reactivity of the former. The different synthesized complexes were compared under the same conditions (entries 6-13), all were less active except **[Mn(L^{Ph})Br_2]** and **[Mn(L^{Cy})Br_2]** which are nearly as efficient as **[Mn(L^{Et})Br_2]. [M(L^{Cy})$_2Cl_2$] (M=Fe, Co)** with two ligands in the coordination sphere of the metal were the less active ones. The better performance of **L^{Et}** supported catalysts compared to **L^{Ph}** ones may be explained by the stronger electron-donating ability of the iminophosphorane function when the phosphorus is substituted by alkyl groups. For quinoline-phosphine cobalt catalysts no hydrosilylation of ketones occurred with the PPh_2 ligands as opposed to $P(^{i}Pr)_2$ ones.[25] The difference between **L^{Cy}** and **L^{Et}** complexes could be due to a greater steric hindrance. Although poorly documented for catalytic applications of iminophosphorane ligands, the steric influence of the phosphorus substituents has already been discussed in coordination experiments.[26]

Also, the influence of the ligand appeared stronger in the Co than Mn series (compare entries 6, 8, 10 and 7,9, 11). The catalytic reaction was optimized with both **[Co(L^{Et})Cl_2]** and **[Mn(L^{Et})Br_2]**, no better results were obtained by adding a cosolvent, nor changing the nature or the quantity of base (see tables S2 and S3). We suspect the cosolvent to compete with isopropanol for metal coordination which slows down the catalysis. Blank experiments were also conducted: no reaction occurred in the absence of the catalyst and base nor in presence of **[Co(L^{Et})Cl_2]** without a base (entries 14, 16). With only **[Mn(L^{Et})Br_2]** the NMR yield was very low (entries 17). The metal precursors under the same conditions led to much less alcohol (entries 18-19). Moreover, ^{t}BuOK alone led to a modest conversion (entry 15).[27] To verify that the catalyst remains active after a catalytic run, one equivalent of acetophenone was added to the reaction mixture after 91% and 96% of phenylethanol had been formed using **[Co(L^{Et})Cl_2]** and **[Mn(L^{Et})Br_2]** respectively. After 24h, only 3% and 13% acetophenone remained with respectively the cobalt and the manganese catalysts (Figure S22,23). This therefore confirms that the catalyst was not destroyed after a catalytic run, nevertheless the Mn complex seems slightly more sensitive than the Co one.

Table 1 : Optimization study for the transfer hydrogenation of acetophenone

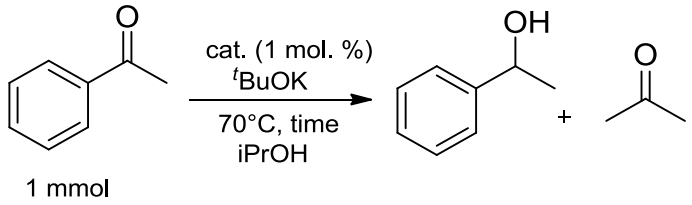

Entry	Cat.	^{t}BuOK (mol%)	^{i}PrOH. (mmol)	Time (h)	NMR yield[a] (%)
1	**[Fe(L^{Et})Cl_2]**	20	30[b]	6	58
2	**[Co(L^{Et})Cl_2]**	20	30[b]	6	23
3	**[Mn(L^{Et})Br_2]**	20	30[b]	6	20
4	**[Co(L^{Et})Cl_2]**	20	30[b]	24	80
5	**[Mn(L^{Et})Br_2]**	20	30[b]	24	56
6	**[Co(L^{Et})Cl_2]**	20	5[c]	24	**91**
7	**[Mn(L^{Et})Br_2]**	20	5[c]	24	**96**
8	**[Co(L^{Ph})Cl_2]**	20	5[c]	24	72
9	**[Mn(L^{Ph})Br_2]**	20	5[c]	24	91
10	**[Co(L^{Cy})Cl_2]**	20	5[c]	24	75
11	**[Mn(L^{Cy})Br_2]**	20	5[c]	24	93
12	**[Fe(L^{Cy})$_2Cl_2$]**	20	5[c]	24	50
13	**[Co(L^{Cy})$_2Cl_2$]**	20	5[c]	24	46
14	none	0	5[c]	24	0
15	none	20	5[c]	24	38
16	**[Co(L^{Et})Cl_2]**	0	5[c]	24	0
17	**[Mn(L^{Et})Br_2]**	0	5[c]	24	6
18	$CoCl_2$	20	5[c]	24	38
19	$MnBr_2$	20	5[c]	24	42

[a] determined by NMR using the integration of the doublet at 1.50 ppm for $CH_3CH(OH)$ relative to the CH aromatic resonances of the reference at 6.10 ppm. [b] concentration 0.41 M. [c] Concentration 2 M.

The scope of the reaction was then studied using the established optimized conditions (Scheme 4). Substituted acetophenones were converted efficiently with both catalysts (**8b-e**), the yield did not change when the methoxy group was located in *ortho* position, which suggests that steric hindrance does not play a prominent role. Of note, lower yields were obtained from p-methoxyacetophenone even after increasing the reaction temperature. Moreover, the yields obtained for **8d** at 70°C with **[Co(L^{Et})Cl_2]** and **[Mn(L^{Et})Br_2]** (54 and 58% respectively) are lower than those from p-trifluoroacetophenone showing an electronic effect of the substituent. P-cyanoacetophenone (**7n**) led to much lower yields (Scheme S2) which may be explained by the coordinating ability of the

substituent. Extending the alkyl chain on the acetophenone as in **8f** did not impact the yield. Considering aliphatic ketones: cyclohexanol **8g** was formed in high yield with both catalysts. High yields were also obtained for 4-*tert*-butylcyclohexanol (**8h**), 2-adamantanol (**8i**), and 2-decanol (**8**j), heptan-2-ol (**8k**), hexan-1-ol (**8l**). The yields for 2-undecanol (**8m**) was slightly lower but still very good with both catalysts. However, 2,6-dimethylcyclohexanone, heptan-4-one, and 2,6-dimethylheptan-4-one did not convert (Scheme S2).

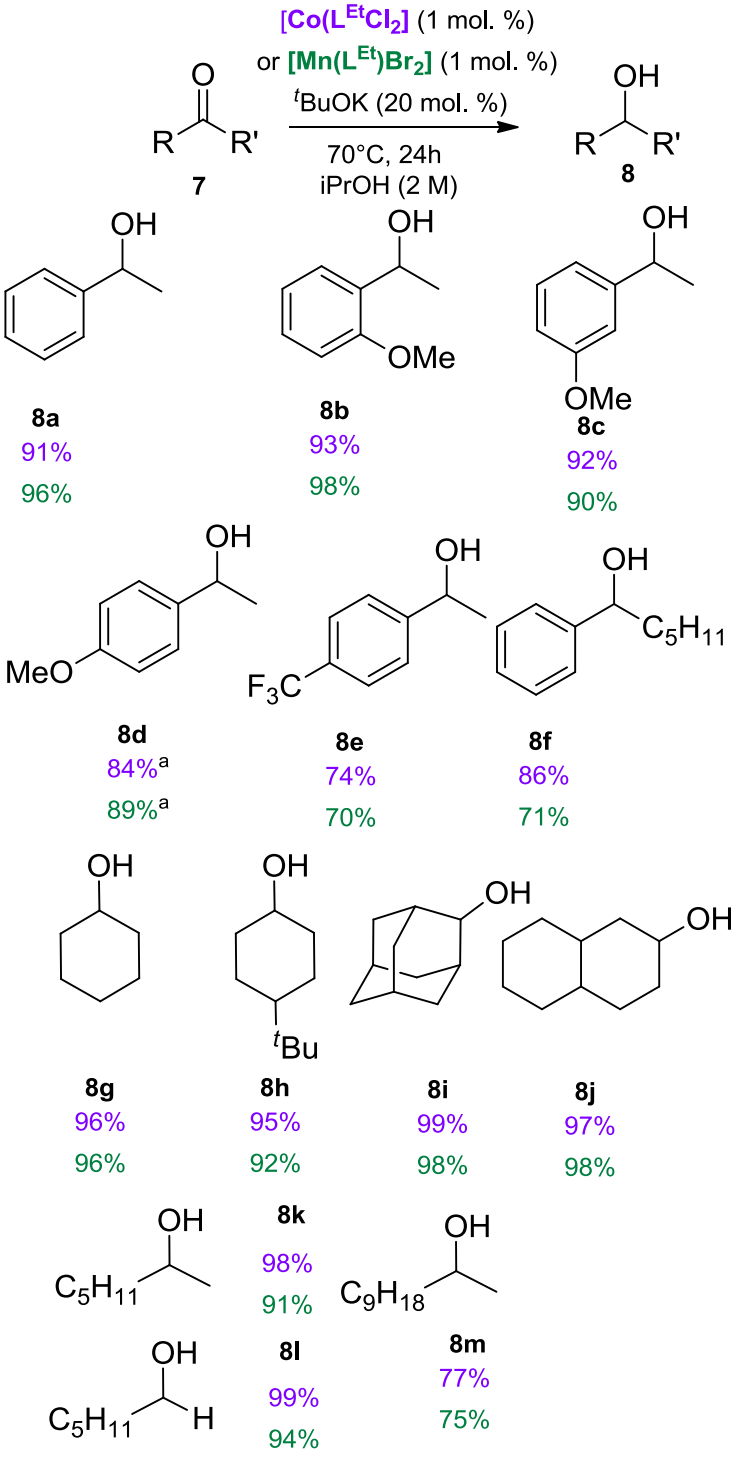

Scheme 4: The substrate scope of the Co^{II} and Mn^{II} catalyzed transfer hydrogenation of ketones. NMR yields determined using trimethoxybenzene as reference are indicated in purple when performed with **[Co(L^{Et})Cl_2]** and **[Mn(L^{Et})Br_2]** in green . [a] Reaction conducted at 90°C.

Therefore, **[Co(L^{Et})Cl_2]** and **[Mn(L^{Et})Br_2]** are efficient for the reduction of aliphatic cyclic ketones provided there is no steric hindrance β to the carbonyl. They are also effective for aliphatic methyl ketones but not with aliphatic substrates exhibiting two acyclic alkyl chain (≥C3). Moreover, heteroaryl-methylketones led to much lower yields even when conducting the reaction at 90°C (Scheme S2), the coordinating ability of this substrate may be at the origin of the problem. To prove this assumption, a competitive experiment in which 4-acetyl-pyridine **7r** and acetophenone **7a** (1 equiv. each) were placed in the catalytic conditions (Scheme S3). Almost no conversion was observed for **7a** (Figure S24, 25), which demonstrates that the catalytic ability of [**Co(L^{Et})Cl_2]** and **[Mn(L^{Et})Br_2]** is inhibited by the presence of **7**r. None of the complex were able to hydrogenate an ester or an amide under the optimized conditions. When comparing the performances of both complexes, no clear conclusion can be drawn, they performed generally very similarly, apart from **8f** for which the cobalt catalyst **[Co(L^{Et})Cl_2]** was slightly better. Compared to the only other Mn^{II} catalyst for transfer hydrogenation of ketones described in the literature,[8] **[Mn(L^{Et})Br_2]** is less efficient for the conversion aromatic ketones, but it delivered aliphatic alcohols with higher efficiency. It is also the unique example of Mn^{II} catalyst involving an iminophosphorane ligand. Regarding cobalt catalysts, the performances of **[Co(L^{Et})Cl_2]** are comparable or better than most previous Co catalysts.[11] However, the catalysts reported by Hanson and Zuo (see Chart 1)[9-10] work at room temperature, with a larger scope for the cationic MACHO Co^{II} complex than the N_2P_2 Co catalyst.

Transfer hydrogenation reactions are known to involve M-H active species that can react with the ketone in an inner or outer sphere mechanism with or without ligand assistance.[28] Therefore, we were interested in proving the formation of such M-H species in the conditions of the reaction. This was challenging because of the paramagnetism of **[Co(L^{Et})Cl_2]** and **[Mn(L^{Et})Br_2]** and only indirect evidences could be obtained. The precatalysts **[Co(L^{Et})Cl_2]** and **[Mn(L^{Et})Br_2]** were reacted with one or two equivalents of $KHBEt_3$ in d_8-THF. In both cases the reaction was sluggish at room temperature, therefore the reaction mixture was heated at 70°C for 1h. A reaction occurred since the initially insoluble halide complexes became soluble and this was accompanied by a color change from a pale lilac suspension to a black solution for **[Co(L^{Et})Cl_2]** and from a pale-yellow suspension to a brown solution for **[Mn(L^{Et})Br_2]**. In the latter case, the reaction mixture could be directly analyzed by ^{1}H NMR spectroscopy, the spectrum displays signals between – 5 and 20 ppm (Figures S60,61). Before the reaction almost no resonance (except those of the solvent) could be seen. No major difference was observed on the spectrum by using 2 equivalents of the hydride donor (Figure S62). From **[Co(L^{Et})Cl_2]**, no ^{1}H NMR spectrum could be recorded because it was impossible to lock. All attempts to isolate the formed products failed, because evaporation of the solvent led to decomposition. Crystallization attempts by diffusion of apolar solvents into the reaction mixture also failed to produce single crystals. As it is impossible to assess the formation of a Mn-H complex based on the poorly informative ^{1}H NMR spectrum obtained, some drops of CCl_4 were added[29] in order to have an indirect proof of the formation of a Mn-H complex through the formation of $CHCl_3$. This led to the observation a singlet at 7.89 ppm (Scheme 5 (i) and Figure S65). The same was done with **[Co(L^{Et})Cl_2]** and a signal that may correspond to $CHCl_3$ was also observed (Figure S66). This suggests the involvement of a M-H species. Then, in order to evaluate if the formed product is an active catalyst for the reaction, it was formed as described previously and placed in the catalytic conditions (corresponding to Table S2-3 entry 6). From **[Co(L^{Et})Cl_2]** and **[Mn(L^{Et})Br_2],** 95% and 91% of 1-phenylethanol respectively was formed after 24h at 70 °C when generating the hydride with $KHBEt_3$

(Scheme 5 (ii)). Not only is the formed hydride species an active catalyst but it worked faster than the one generated from isopropanol and the base because these catalytic conditions led to 48% and 68% of phenylethanol. It therefore suggests an induction period for the formation of the hydride species with only ^{t}BuOK and isopropanol. It was then necessary to determine whether the presence of a hydride species could be detected indirectly in the employed catalytic conditions. **[Co(L^{Et})Cl_2]** and **[Mn(L^{Et})Br_2]** were reacted with isopropanol (500 equiv.) and ^{t}BuOK (20 equiv.) during 4h at 70°C, then some drops of CCl_4 were introduced and after some minutes some THF-d_8 to allow the recording of a ^{1}H NMR spectrum (Scheme 5 (iii)). In each case, a weak signal that may correspond to $CHCl_3$ was observed (Figures S57,58). This reaction of *in-situ* generated hydride species should prevent any catalysis in presence of a halogenoalkane. As shown in Scheme S4, no catalysis occurred with either catalyst in presence of 1 mol. % $CDCl_3$ which reinforces the idea that metal-hydride species is involved in this reaction. Then, the potential interaction of a ketone with the *in situ* generated M-H complex formed with $KHBEt_3$ was investigated. This experiment was conducted from **[Mn(L^{Et})Br_2]** for which it was possible to lock contrary to solutions of **[Co(L^{Et})Cl_2]**. The hydride species was formed as described previously and then acetophenone was added (Scheme 5 (iv)). The ^{1}H NMR spectrum recorded just after the addition showed the presence of free acetophenone (in particular a singlet at 2.58 ppm in THF-d_8, Figure S67). After 1 h at 70°C this signal has disappeared and the other signals have changed. This may suggest an interaction between the metal species and the acetophenone. No single crystal could be grown from this solution and the ^{1}H NMR data are not as informative as with a diamagnetic complex preventing to draw any conclusion about the nature of this interaction (coordination/insertion or outer sphere interaction). Nevertheless, the experiments carried out suggest the formation of a M-H species in the catalytic conditions and the existence of an interaction between it and the substrate.

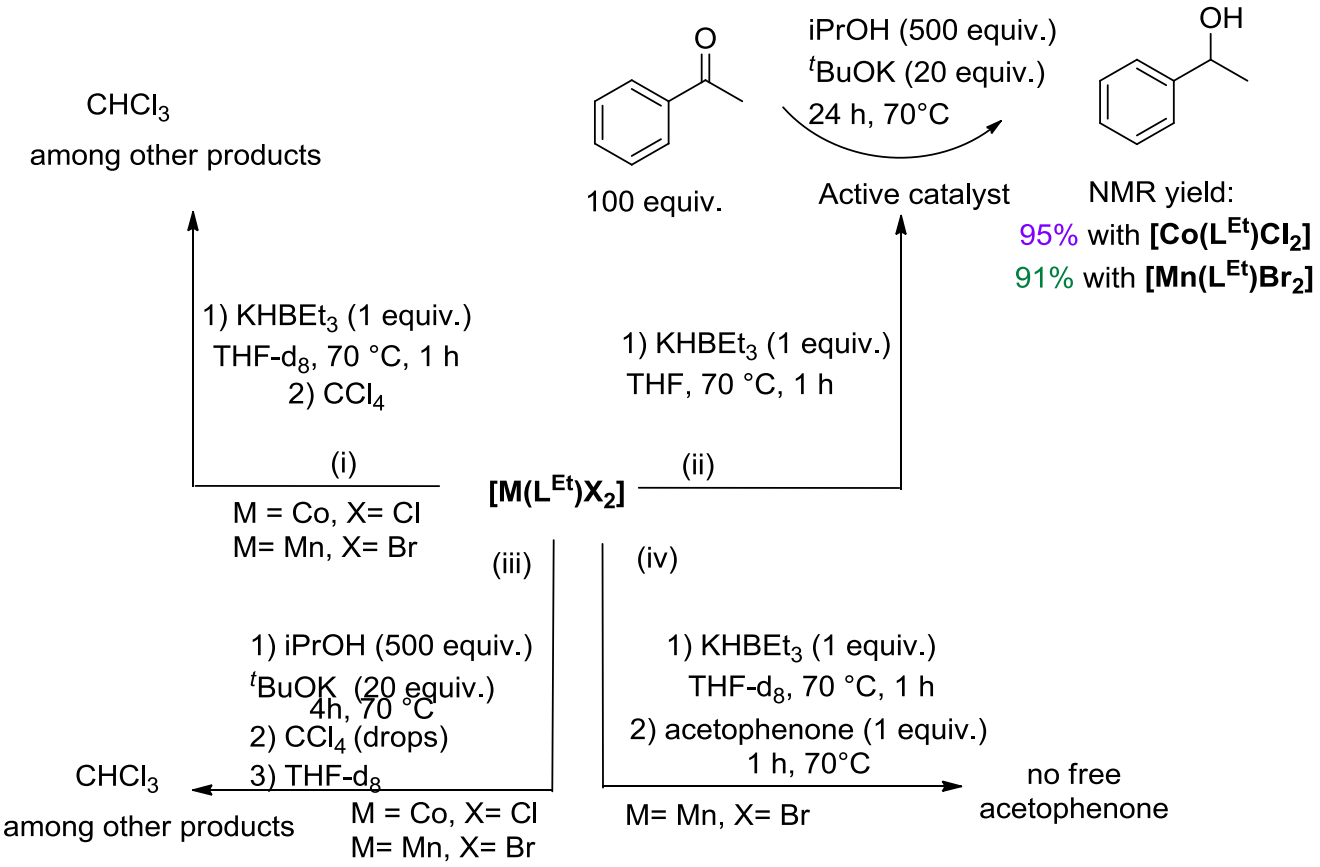

Scheme 5: Experiments to get insights into the reaction mechanism

3. Conclusion

Three tridentate NNN ligand associating a pyridine, a secondary amine, and an iminophosphorane differing by the substituents of the P atom were synthesized. They were coordinated to Fe^{II}, Co^{II}, and Mn^{II} metal centers leading in moderate to high yields to the corresponding high-spin complexes. In the case of the tris(cyclohexyl) P-substituted ($\mathbf{L^{Cy}}$), ligand scrambling was shown at least for the Fe^{II} and Co^{II} complexes. This process was shown to require several days to go to completion. The performances of Co^{II} and Mn^{II} complexes were compared for transfer hydrogenation reaction of ketones, for which these metals remain underexploited. $\mathbf{L^{Et}}$ supported complexes were the most efficient. They produced good to very good yields of alcohols after one day at 70°C from substituted phenones and dialkylketones. Noteworthily, Co^{II} and Mn^{II} catalysts supported by an iminophosphorane ligand are almost unprecedented for this reaction (only one poorly active Co catalyst was previously reported). Even if these catalysts require heating they proved more efficient that the majority of the previous examples in particular to convert aliphatic ketones. In addition, it represents, to the best of our knowledge, the first study where analogous Co^{II} and Mn^{II} catalysts are compared. In order to get some insights into the reaction mechanism and despite the paramagnetism of the catalysts, some experiments were conducted suggesting the involvement of hydride species in catalytic conditions and the ability of the latter to interact with the substrate. This study validates the idea that Co^{II} and Mn^{II} metals, which have been rarely or never used in combination with iminophosphorane ligands to develop catalysts, deserve more attention. More

generally, while a myriad of Mn^{I} carbonyl catalysts have emerged in organometallic catalysis in the past few years, Mn^{II} ones remains underemployed. However, Mn^{II} metal precursors are much cheaper than Mn^{I} carbonyl ones, so their use should increase. To that end, iminophosphorane ligands may be an asset

4. Experimental Section

4.1 General information

All air and moisture sensitive reactions were performed under inert atmosphere using a vacuum line, inert Schlenk techniques (N_2) and a glove box (Ar, <0.1 ppm H_2O, <0.1 ppm O_2) with oven-dried glassware unless other notified. Reagents were used as received from commercially available suppliers without further purification unless otherwise noticed. CH_2Cl_2, pentane, and toluene were taken from solvent purification system (MBraun-SPS). THF, ^{i}PrOH, and Et_2O were distilled over Na and degassed using freeze-pump technique. NMR spectra were recorded on a Bruker AC-300 SY spectrometer at 300 MHz for ^{1}H, 120 MHz for ^{31}P and 75 MHz for ^{13}C. Solvent peaks were used as internal references for ^{1}H and ^{13}C chemical shifts (ppm). $^{31}P\{^{1}H\}$ NMR spectra are relative to an 85% H_3PO_4 external reference. Unless otherwise mentioned, NMR spectra were recorded at 300 K. The spectra were analyzed with Topspin software. The following abbreviations are used: s, singlet; d, doublet; dd, doublet of doublets; t, triplet; m, multiplet. Mass spectrometry experiments were performed on a Tims-TOF mass spectrometer (Bruker, France) equipped with two ionization sources: Electrospray (ESI) and chemical ionization at atmospheric pressure (APCI). All mass spectra were produced in positive mode. Samples were prepared in acetonitrile at µM concentration. 2 µL were introduced into the interface of the instrument without separation using an Elute UHPLC module (Bruker) at a 100 µL min^{-1} flow rate. Capillary and end plate voltages were set at 4.2 kV and 0.5 kV for experiments, Corona for APCI was set at 4000nA. Nitrogen was used as the nebulizer and drying gas at 2 bar and 8 L min^{-1}, respectively, with a drying temperature of 220 °C. APCI heater was set at 300°C. Tuning mix (Agilent, France) was used for calibration. The elemental compositions of all ions were determined with the instrument software Data Analysis, the precision of mass measurement was less than 4 ppm. Elemental analyses were performed by the elemental analysis service of the Laboratoire de Chimie de Coordination (Toulouse) using a PerkinElmer 2400 series II analyzer. X-ray crystallography data were collected at 150 K on a Bruker Kappa APEX II diffractometer for **1**, **[Fe(L^{Et})Cl_2]**, and **[Fe(L^{Cy})$_2Cl_2$]**, or a Stoe Stadivari diffractometer for **L^{Ph}**, **[Co(L^{Et})Cl_2]**, **[Mn(L^{Et})Br_2]**, and **[Co(L^{Cy})$_2Cl_2$]** using a Mo-κ (λ = 0.71069Å) X-ray source and a graphite monochromator. The crystal structures were solved using Shelxt33[30] or olex[31] and refined using Shelxl-97 or Shelxl-2014.[32] ORTEP drawings were made using ORTEP III[33] for Windows. Details of crystal data Details of crystal data and structure refinements are summarized in Tables S3-4.

4.2 Syntheses

Synthesis of 1: 2-picolylamine (1.39 g, 12.85 mmol, 10 equiv.) is added to a solution of 1-Azido-2- (bromomethyl)benzene (277.5 mg, 1.285 mmol) in CH_2Cl_2 (10 mL) at 0°C. The reaction progress was followed by TLC ($rf_{product}$ = 0.4, eluent 3: 1 EtOAc/Pentane) and the reaction finished within 1h30. The mixture was quenched with water (20 mL) and the organic phase was extracted with EtOAc (3 x 10 mL) and washed with brine (1 x 20 mL). The organic phase was dried over MgSO4 filtered and concentrated under vacuum. The compound was purified by column chromatography (eluent 3: 1 EtOAc/Pentane), after evaporation of the solvent, **1**

was isolated as a brown oil (0.2585 g, 1.08 mmol, 84%).1H NMR (CD_2Cl_2, 300 MHz, 25°C) : δ = 8.51 (m, 1H, H_{pyr}), 7.64 (dt, $J_{H,H}$ = 7.7,2.0 Hz, H_{Pyr}), 7.39- 7.28 (m, 3H, $H_{Ar,}$ H_{Pyr}), 7.18-7.12 (m, 3H, $H_{Ar\ +\ Pyr}$), 3.86 (s, 2H, CH2), 3.76 (s, 2H, CH2), 2.06 (bs, 1H, NH). 13C{1H} NMR (CD_2Cl_2, 75.5 MHz, 25°C) : δ = 160.6 (C), 149.6 (CH_{Ar}), 138.7 (C), 136.7 (CH_{Ar}), 132.2 (C), 130.7 (CHAr, 128.8 (CH_{Ar}), 125.2 (CH_{Ar}), 122.5 (CH_{Ar}), 122.3 (CH_{Ar}), 118.6 (CHAr), 55.0 (CH_2Pyr), 49.3 (CH_2). HRMS (APCI$^+$): *m/z* calculated for $[C_{13}H_{14}N_5]^+$ ([1].H^+): *m/z* 240.1243; found: *m/z* 240.1235.

Synthesis of L^{Et}: A solution of PEt_3 (62.2 mg, 0.5265 mmol) in Et_2O (1 mL) was added to a solution of the **1** (0.126 g, 0.5265 mmol) in Et_2O (3 mL) leading to a gaseous evolution while the solution turned brown. The reaction was completed after 24 h at room temperature as confirmed by ^{31}P NMR. The solvent was removed in vacuo to yield **L^{Et}** as a brown solid (0.146 g, 0.443 mmol, 84%) after washing with pentane (2 x 3 mL). ^{31}P NMR ($CDCl_3$, 121.5 MHz, 25°C) : δ = 22.8 ppm; ^{1}H NMR ($CDCl_3$, 300 MHz, 25°C) : δ = 8.68 (ddd, $J_{H,H}$ = 4.9, 1.9, and 0.9 Hz, 1H, CH_{pyr}), 7.77 (td, $J_{H,H}$ = 7.5 and 2.0 Hz, 1H), 7.56 (dt, $J_{H,H}$ = 7.5 and 2.0 Hz, 1H), 7.31-7.23 (m, 2H), 7.13 (td, $J_{H,H}$ = 7.5 and 2.0 Hz, 1H), 6.80-6.74 (m, 1H), 6.70 (dt, $J_{H,H}$ = 7.5 and 1.5 Hz, 1H), 4.04 (s, 2H), 4.03 (s, 2H), 3.43 (bs, 1H, NH), 1.87 (dq, 2 $J_{P,H}$ = 11.5 Hz, 6H), 1.13 (dt, 3 $J_{P,H}$ = 15.8 Hz); ^{13}C{^{1}H} NMR ($CDCl_3$, 75.5 MHz, 25°C) : δ = 161.3 (C), 151.1 (d, $J_{P,C}$ = 3.5 Hz, C), 149.1 (CH_{Ar}), 136.1 (CH_{Ar}), 133.1 (d, $J_{P,C}$ = 20.5 Hz, C), 129.9 (d, $J_{P,C}$ = 2.0 Hz, CH_{Ar}), 127.3 (CH_{Ar}), 122.1 (CH_{Ar}), 121.4 (CH_{Ar}), 120.1 (CH_{Ar}), 116.4 (CH_{Ar}), 54.8 (CH_{2Pyr}), 52.9 (CH_2), 19.1 (d, $J_{P,C}$ = 63.5 Hz, CH_{2Et}), 6.4 (d, $J_{P,C}$ = 4.5 Hz, CH_{3Et}). HRMS (APCI$^+$): calculated for $[C_{19}H_{29}N_3P]^+$ ([**L^{Et}**].H^+): *m/z* 330.2090; found: *m/z* 330.2093. Elemental analysis for $C_{19}H_{28}N_3P$: calc (%) C 69.27; H 8.57; N 12.76; found (%) C 69.48; H 8.57; N 13.10.

Synthesis of L^{Cy}: A solution of PCy_3 (0.337 g, 1.2 mmol) in of Et_2O (5 mL) to a solution of **1** (0.287 g, 1.2 mmol) in THF (7 mL), leading to a gaseous evolution while the solution turned brown. The reaction was completed within 24 h at room temperature as confirmed by ^{31}P NMR. The solvent was evaporated, and the residue was washed with pentane (2 x 10 mL) to yield **L^{Cy}** as a brown solid (0.412 g, 0.8899 mmol, 72%). ^{31}P NMR (THF-d_8, 121.5 MHz, 25°C) : δ = 20.5 ppm; ^{1}H NMR (THF-d_8, 300 MHz, 25°C) : δ = 8.40 (m, 1H, $J_{H,H}$ = 4.5 and 1.0 Hz, CH_{pyr}), 7.85 (td, $J_{H,H}$ = 7.5 and 1.0 Hz, 1H), 7.48 (d, $J_{H,H}$ = 7.6 Hz, 1H), 7.04 (m, 1H, $J_{H,H}$ = 7.5 and 4.5 Hz), 6.96 (dt, $J_{H,H}$ = 7.5 and $J_{P,H}$ = 2.0 Hz, 1H), 6.81 (td, $J_{H,H}$ = 7.5 and $J_{P,H}$ = 2.0 Hz, 1H), 6.48 (d, $J_{H,H}$ = 7.5 Hz, 1H), 6.38 (t, $J_{H,H}$ = 7.5 Hz, 1H, CHAr), 3.69 (s, 2H; CH_2), 3.63 (s, 2H, CH_2), 3.47 (bs, 1H, NH), 2.20 ppm (3H, CH_{Cy}, $J_{P,H}$ = 10.0 Hz) 2.05-1.12 (m, 30H, H_{Cy}); ^{13}C{^{1}H} NMR (THF-d_8, 75.5 MHz, 25°C) : δ = 163.3 (C), 152.6 (d, $J_{P,C}$ = 3.0 Hz, C), 149.6 (CH_{Ar}), 136.4 (CH_{Ar}), 134.2 (d, $J_{P,C}$ = 21.5 Hz, C) , 130.0 (d, $J_{P,C}$ = 2.5 Hz, CH_{Ar}) , 127.5 (CH_{Ar}), 122.2 (CH_{Ar}), 121.7 (CH_{Ar}), 120.8 ($J_{P,C}$ = 6.5 Hz, CH_{Ar}) , 115.8 (CH_{Ar}), 56.1 (CH_{2Pyr}), 54.5 (CH_2), 37.96 (d, $J_{P,C}$ = 58.5 Hz, CH_{Cy}), 28.6 (d, $J_{P,C}$ = 3.5 Hz, CH_{2Cy}), 28.19 (d, $J_{P,C}$ = 12.5 Hz, CH_{2Cy}), 27.2 (CH_{2Cy}). HRMS (APCI$^+$): calculated for $[C_{31}H_{47}N_3P]^+$ ([**L^{Cy}**].H^+): *m/z* 492.3502; found: *m/z* 492.3492. Elemental analysis for $C_{31}H_{46}N_3P$ (0.1 CH_2Cl_2): calc (%) C 74.68; H 9.43; N 8.55; found (%) C 74.82; H 9.28; N 9.12. $C_{31}H_{46}N_3P$ 0.1 CH2Cl2: calc (%) C 74.68; H 9.31; N 8.40;

Synthesis of L^{Ph}: A solution of PPh_3 (0.134, 0.511 mmol) in toluene (1 mL) was added to a solution of **1**(0.124 g, 0.511 mmol) in toluene (5 mL) leading to a gaseous evolution. A precipitate appeared after 1 h of stirring. The reaction is left to stir at room temperature for 24 h. The mixture was concentrated to favor the precipitation and then filtered to collect the solid. More product was obtained by addition of pentane (5 mL) to the filtrate. Both solids were collected and washed with pentane (2 x 3 mL) to yield **L^{Ph}** as a white solid (0.241, 0.480 mmol, 94 %). ^{31}P NMR (THF-d_8, 121.5 MHz, 25°C) : δ = 0.1 ppm; ^{1}H NMR (THF-d_8, 300 MHz, 25°C) : δ = 8.39 (m, 1H, CH_{pyr}), 7.84-7.77 (m, 6H, CH_{Ar}), 7.54-7.42 (m, 10H, CH_{Ar} + 2 CH_{Pyr}), 7.31 (m, 1H, CH_{Ar}), 7.11-7.02 (m, 2H, CH_{Ar} + CH_{Pyr}), 6.63 (m, 1H, CH_{Ar}), 6.47 (m, 1H, CH_{Ar}), 6.37 (m, 1H, CH_{Ar}), 3.99 (s, 2H, CH_2), 3.89 (s, 2H, CH_2), 2.48 (bs, 1H, NH); ^{13}C{^{1}H} NMR (THF-d_8, 75.5 MHz, 25°C) : δ = 163.0 (C), 150.4 (d, $J_{P,C}$ = 1.5 Hz, C), 149.7 (CH_{Ar}), 136.5 (CH_{Ar}), 135.2 (d,

$J_{P,C}$ = 22.0 Hz, C), 134.6 (d, $J_{P,C}$ = 20.0 Hz, CH_{Ar}), 133.5 (d, $J_{P,C}$ = 9.5 Hz, CH_{Ar}), 132.9 (d, $J_{P,C}$ = 2.5 Hz, C), 132.4 (CH_{Ar}), 130.1 (d, $J_{P,C}$ = 2.5 Hz, CH_{Ar}), 129.5 (d, $J_{P,C}$ = 12.0 Hz, CH_{Ar}), 129.4 (CH_{Ar}) , 127.5 (CH_{Ar}), 122.4 (CH_{Ar}), 121.9 (CH_{Ar}), 121.6 (d, $J_{P,C}$ = 10.5 Hz, CH_{Ar}), 117.6 (CH_{Ar}), 56.0 (CH_{2Pyr}), 53.5 (CH_2). HRMS ($APCI^+$): calculated for $[C_{31}H_{29}N_3P]^+$ ($[\mathbf{L^{Ph}}].H^+$): *m/z* 474.2094; found: *m/z* 474.2090. Elemental analysis for $C_{31}H_{28}N_3P$ (0.6 C_5H_{12}): calc (%) C 79.01; H 6.86; N 8.13; found (%) C 79.48; H 6.91; N 8.56.

Synthesis of [Fe($\mathbf{L^{Et}}$)$\mathbf{Cl_2}$]: A solution of $FeCl_2$ (56 mg, 0.371 mmol) in THF (1 mL) was slowly added to a solution of $\mathbf{L^{Et}}$ (122 mg, 0.371 mmol) in THF (3 mL). After 24h at room temperature a precipitate had formed. The mixture was concentrated until 1 mL to favor the precipitation and was filtered, the precipitate was washed with THF (2x2 mL) and dried under vacuum to give a green solid (72 mg, 0.157 mmol, 42%). ^{1}H NMR (CD_2Cl_2, 300 MHz, 25°C) : δ = 191.35 (s , 1H), 100.91 (s , 1H), 56.74 (s , 1H), 33.27 (s , 1H), 14.54 (s , 1H), 11.09 (s , 1H), 6.15 (s , 1H), 1.64 (s , 1H), -0.07 (s , 15H), -3.92 (s , 1H), -8.66 (s , 1H), -1.49 (s , 2H), -19.67 (s , 1H). Evans method (C = 12.9 mM; CD_2Cl_2): 5.22 μ_B, S = 2. HR-MS (ESI^+): calculated for $[C_{19}H_{28}ClFeN_3P]^+$ ($[M\text{-}Cl]^+$): *m/z* 420.1053; found *m/z* 420.1057. Elemental analysis for $C_{19}H_{28}N_3PFeCl_2$ (0.05 CH_2Cl_2): calc (%) C 49.70; H 6.15; N 9.13; found (%) C 49.79; H 6.11; N 9.34.

Synthesis of [Fe($\mathbf{L^{Cy}}$)$\mathbf{Cl_2}$]: A solution of $FeCl_2$ (27.6 mg, 0.219 mmol) in THF (1 mL) was slowly added to a solution of $\mathbf{L^{Cy}}$ (113.4 mg, 0.219 mmol) in THF (2 mL). After 24h at room temperature a precipitate had formed. The mixture is concentrated until 1 mL to favor the precipitation and was then filtered. The precipitate was washed with THF (2x2 mL) and dried under vacuum to give a green solid (70 mg, 0.114 mmol, 52%). ^{1}H NMR (CD_2Cl_2, 300 MHz, 25°C) : δ = 128.00 (s , 1H), 94.72 (s , 1H), 47.28 (s , 1H), 35.19 (s , 1H), 13.64 (s , 2H), 9.21 (s , 2H), 4.03-4.59 (m , 6H), 0.97-1.30 (m , 12H), -3.94-(-2.11) (m , 12H), -7.40-(-6.42) (m , 2H), -11.59-(-10.81) (m , 3H). Evans method (C = 6.2 mM; CD_2Cl_2): 4.94 μ_B, S = 2. HRMS ($APCI^+$): $[C_{31}H_{46}ClFeN_3P]^+$ ($[M\text{-}Cl]^+$): *m/z* 582.2462; found *m/z* 582.2469. Elemental analysis for $C_{31}H_{46}N_3PFeCl_2$ (0.1 CH_2Cl_2): calc (%) C 59.58; H 7.43; N 6.70; found (%) C 59.80; H 7.19; N 6.25.

Synthesis of [Fe($\mathbf{L^{Ph}}$)$\mathbf{Cl_2}$]: A solution of $FeCl_2$ (23.7mg, 0.188 mmol) in THF (1 mL) was slowly added to a solution of $\mathbf{L^{Ph}}$ (89.2 mg, 0.188 mmol) in THF (2 mL). After 24h at room temperature a precipitate had formed, the mixture was concentrated until 1 mL to favor the precipitation and was then filtered. The precipitate was washed with THF (2x2 mL) and dried under vacuum to give a green solid (77 mg, 0.130 mmol, 69%).^{1}H NMR (CD_2Cl_2, 300 MHz, 25°C) : δ = 122.75 (s , 1H), 95.88 (s , 1H), 53.72 (s , 1H), 50.00 (s , 1H), 31.67 (s , 1H), 12.49 (s , 1H), 10.36 (s , 5H), 8.83 (s , 1H), 7.73 (s , 6H), 6.09 (s , 3H), 0.87-1.26 (m , 4H), -1.97 (s , 1H), -5.30 (s , 2H). Evans method (C = 5.7 mM; CD_2Cl_2): 4.92 μ_B, S = 2. HRMS ($APCI^+$): $[C_{31}H_{28}ClFeN_3P]^+$ ($[M\text{-}Cl]^+$): *m/z* 564.1054; found *m/z* 564.1053. Elemental analysis for $C_{31}H_{28}N_3PFeCl_2$: calc (%) C 62.02; H 4.70; N 7.00; found (%) C 61.85; H 4.44; N 6.77.

Synthesis of [Co($\mathbf{L^{Et}}$)$\mathbf{Cl_2}$]: A suspension of $\mathbf{L^{Et}}$ (248.7 mg, 0.75 mmol) and $CoCl_2$ (97.4 mg, 0.75 mmol) in THF (8 mL) was stirred at room temperature for 16h. The grey suspension turned to a purple one. The solid was separated and dried under vacuum to give **[Co($\mathbf{L^{Et}}$)$\mathbf{Cl_2}$]** (262.3 mg, 0.58 mmol, 77%). ^{1}H NMR (CD_2Cl_2, 300 MHz, 25°C) : δ = 229.63 (s , 1H, CH), 140.73 (s , 1H, CH), 73.29 (s , 1H, CH), 48.26 (s , 2H), 44.03 (s , 2H), 26.41 (s , 3H), 21.11 (s , 2H), -2.93-0.09 (m , 6H, $CH_{2\ Et}$), -7.12 (s , 9H, $CH_{3\ Et}$), -227.77 (s , 1H). Evans method (C = 15.6 mM; CD_2Cl_2): 4.32 μ_B, S = 3/2. HRMS ($APCI^+$): $[C_{19}H_{28}ClCoN_3P]^+$ ($[M\text{-}Cl]^+$): *m/z* 423.1035; found *m/z* 423.1020. Elemental analysis for $C_{19}H_{28}N_3PCoCl_2$ (0.2 CH_2Cl_2): calc (%) C 48.42; H 6.01; N 8.82; found (%) C 48.23; H 5.78; N 8.99.

Synthesis of [Co($\mathbf{L^{Cy}}$)$\mathbf{Cl_2}$]: A suspension of $\mathbf{L^{Cy}}$ (245.8 mg, 0.5 mmol) and $CoCl_2$ (65.0 mg, 0.5 mmol) in THF (6 mL) was stirred at room temperature for 16h. The grey suspension turned to a blue one. The solid was separated and dried under vacuum to give **[Co($\mathbf{L^{Cy}}$)$\mathbf{Cl_2}$]** (191.3 mg, 0.31 mmol, 62%). ^{1}H NMR (CD_2Cl_2, 300 MHz, 25°C) : δ = 45.72 (s, 2H), 23.15 (s, 1H), 17.60 (s, 3H), 7.50 (s, 6H, $CH_{2\ Ph}$), 4.69 (s, 9H,

$CH_{2\ Ph\ and}$ CH_{Ph}), 2.78 (s, 1H), 0.19-1.30 (m, 2H), -0.60 (s, 1H), -2.68 (s, 3H). Evans method (C = 8.6 mM; CD_2Cl_2): 4.31 μ_B, S = 3/2. HR-MS (APCI): calculated for $[C_{31}H_{46}ClCoN_3P]^+$ ($[M\text{-}Cl]^+$): *m/z* 585.2444; found *m/z* 585.2461. Elemental analysis for $C_{31}H_{46}N_3PCoCl_2$ (0.1 CH_2Cl_2): calc (%) C 59.29; H 7.39 N 6.67; found C 59.38; H 6.92; N 6.46.

Synthesis of $[Co(L^{Ph})Cl_2]$: A suspension of L^{Ph}(251.1 mg, 0.5 mmol) and $CoCl_2$ (65.0 mg, 0.5 mmol) in THF (6 mL) was stirred at room temperature for 16h. The grey suspension turned to a blue one. The solid was separated and dried under vacuum to give **$[Co(L^{Ph})Cl_2]$** (217.0 mg, 0.36 mmol, 72%). ^{1}H NMR (CD_2Cl_2, 300 MHz, 25°C): δ = 45.72 (s, 2H), 23.15 (s, 1H), 17.60 (s, 3H), 7.50 (s, 6H, $CH_{2\ Ph}$), 4.69 (s, 9H, CH_{2Ph} and CH_{Ph}), 2.78 (s, 1H), 0.19-1.30 (m, 2H), -0.60 (s, 1H), -2.68 (s, 3H). Evans method (C = 11.2 mM; CD_2Cl_2): 4.31 μ_B, S = 3/2. HR-MS (APCI): calculated for $[C_{31}H_{28}ClCoN_3P]^+$ ($[M\text{-}Cl]^+$): *m/z* 567.1036; found *m/z* 567.1056. Elemental analysis for $C_{31}H_{28}N_3PCoCl_2$ (0.25 CH_2Cl_2): calc (%) C 60.09; H 4.60; N 6.73; found (%) C 60.00; H 4.36; N 7.06.

Synthesis of $[Mn(L^{Et})Br_2]$: L^{Et} (331.6 mg, 1.0 mmol) and $MnBr_2$ (214.8 mg, 1.0 mmol) were mixed in THF (8 mL) and stirred at room temperature for 16h. The light-yellow solution became a white suspension and the solid was isolated. After drying in vacuo **$[Mn(L^{Et})Br_2]$** was isolated as a white solid (405.8 mg, 0.71 mmol, 71%). ^{1}H NMR (CD_2Cl_2, 300 MHz, 25°C): δ = 52.90 (m, 8H), 16.16 (s , 3H), 18.89 (s , 2H), -19.07 (s , 15H, CH_{2Et} and CH_{3Et}). Evans method (C= 14.9 mM; CD_2Cl_2): 6.05 μ_B, S = 5/2. HR-MS (APCI): calculated for $[C_{19}H_{28}BrMnN_3P]^+$ ($[M\text{-}Br]^+$): *m/z* 463.0579; found *m/z* 463.0573. Elemental analysis for $C_{19}H_{28}N_3PMnBr_2$: calc (%) C 41.94; H 5.19; N 7.72; found (%) C 42.13; H 4.92; N 7.73.

Synthesis of $[Mn(L^{Cy})Br_2]$: L^{Cy} (248.5 mg, 0.5 mmol) and $MnBr_2$ (107.4 mg, 0.5 mmol) were mixed in THF (6 mL) and stirred at room temperature for 16h giving a light-yellow suspension. After removal of the volatiles the obtained white solid was washed with pentane (2x5 mL). After drying in vacuo **$[Mn(L^{Cy})Br_2]$** was isolated as a white solid (261.7 mg, 0.37 mmol, 74%). ^{1}H NMR (CD_2Cl_2, 300 MHz, 25°C): δ = 44.38-51.29 (m, 4H), 33.73 (s, 4H), 19.60 (s, 18H, CH_{Cy}), -11.74 (s , 12H, CH_{Cy}), -28.56 (s , 5H). Evans method (C = 9.2 mM; CD_2Cl_2): 6.37 μ_B, S = 5/2. HR-MS (APCI): calculated for $[C_{31}H_{46}BrMnN_3P]^+$ ($[M\text{-}Br]^+$): *m/z* 625.1987; found *m/z* 625.1994. Elemental analysis for $C_{31}H_{46}N_3PMnBr_2$: calc (%) C 51.36; H 6.42; N 5.74; found (%) C 50.93; H 6.34; N 6.10.

Synthesis of $[Mn(L^{Ph})Br_2]$: L^{Ph} (50.2 mg, 0.1 mmol) and $MnBr_2$ (21.5 mg, 0.1 mmol) were mixed in THF (2 mL) and stirred at room temperature for 16h giving a light-yellow solution. After removal of the volatiles the obtained white solid was washed with pentane (2x1.5 mL). After drying in vacuo **$[Mn(L^{Ph})Br_2]$**was isolated as a white solid (62.6 mg, 0.08 mmol, 80%). ^{1}H NMR (CD_2Cl_2, 300 MHz, 25°C): δ = 44.38-51.29 (m, 4H), 33.73 (s, 4H), 19.60 (s, 18H, CH_{Cy}), -11.74 (s , 12H, CH_{Cy}), -28.56 (s , 5H). Evans method (C = 9.1 mM; CD_2Cl_2): 5.59 μ_B, S = 5/2. HR-MS (APCI): calculated for $[C_{31}H_{28}BrMnN_3P]^+$ ($[M\text{-}Br]^+$): *m/z* 607.0579; found *m/z* 607.0590. Elemental analysis for $C_{31}H_{28}N_3PMnBr_2$: calc (%) C 54.10; H 4.10; N 6.10; found (%) C 54.09; H 4.21; N 5.81.

Synthesis of $[Fe(L^{Cy})_2Cl_2]$: L^{Cy} (49.2 mg, 0.1 mmol) and $FeCl_2$ (6.4 mg, 0.05 mmol) were mixed in THF (0.6 mL) and stirred at room temperature for 16h. The yellow suspension became a red one. The solid was separated and dried under vacuum to give **$[Fe(L^{Cy})_2Cl_2]$** (30.2 mg, 0.028 mmol, 55%). ^{1}H NMR (CD_2Cl_2, 300 MHz, 25°C: δ = 54.81 (s, 1H), 52.45 (s, 1H), 47.37 (s, 1H), 35.0 (s, 1H), 16.80 (s, 1H), 14.54 (s, 1H), 10.73 (s, 1H), 10.40 (s, 1H), 10.02 (s, 1H), 9.79 (s, 1H), 9.47 (s, 1H), 8.80 (s, 1H), 7.16-7.50 (m, 2H), 6.40 (m, 2H), 4.92 (s, 1H), 3.44 (s, 1H), -1.22-1.45 (m, 66H), -2.06 (s, 1H), -2.51 (s, 1H), -3.25 (s, 2H), -4.80 (s, 1H). Evans method (C = 4.2 mM; CD_2Cl_2): 4.56 μ_B, S = 2. HR-MS (ESI^+): calculated for $[C_{62}H_{92}ClFeN_6P_2]^+$ ($[M\text{-}Cl]^+$): *m/z* 1109.5658; found *m/z* 1109.5659. Elemental analysis for $C_{62}H_{92}N_6PCoCl_2$ (0.4 CH_2Cl_2) : calc (%) C 65.87; H 8.20; N 7.53; found (%) C 66.04; H 9.07; N 8.12.

Synthesis of $[Co(L^{Cy})_2Cl_2]$: L^{Cy} (49.2 mg, 0.1 mmol) and $CoCl_2$ (6.5 mg, 0.05 mmol) were mixed in THF (0.6 mL) and stirred at room temperature for 16h. The grey suspension became a yellow one. The solid was separated and dried under vacuum to give **$[Co(L^{Cy})_2Cl_2]$** (37.7 mg, 0.034 mmol, 68%). ^{1}H NMR (CD_2Cl_2, 300 MHz, 25°C: δ = 145.1 (s, 2H), 48.39 (s, 3H), 41.09 (s, 4H), 34.46 (s, 2H), 26.52 (s, 6H), 18.32 (s, 2H), 13.86 (s, 2H), 12.39 (s, 2H), 0.88-4.055 (m, 66H), -5.14 (s, 1H). Evans method (C = 4.4 mM; CD_2Cl_2): 3.83 μ_B, S = 3/2. Elemental analysis for $C_{62}H_{92}N_6PCoCl_2$ (0.4 CH_2Cl_2) : calc (%) C 65.89; H 8.33; N 7.55; found (%) C 65.90; H 8.71; N 7.19.

General procedure for the transfer hydrogenation of ketones: In the glovebox, the ketone derivative (1 mmol, 1 equiv.), trimethoxy benzene (11.8 mg, 0.07 mmol), and [M(L)Cl] (0.01 mmol, 1 mol%) were successfully introduced in a 6 mL catalytic vial. Then, ^{i}PrOH (0,382 mL, 5 mmol, 5 equiv.) and ^{t}BuOK (22.4 mg, 0.2 mmol, 20 mol%) were added and the vial was capped. After stirring 24h at 70°C, the vials were uncapped and the volatiles were evaporated on the rotary evaporator (30 min, 50 mbar, 40°C). The solution was then quenched with distilled water (1.5 mL), extracted with Et_2O (5.0 mL), and then dried on $MgSO_4$. The solvents were evaporated on the rotary evaporator (15 min, 50 mbar, 40°C) and analyzed by NMR in $CDCl_3$. In the case of **8j-m** because of the poor solubility of the compounds, the extractions were made with EtOAc.

4.3 . Appendix A. Supplementary material

Experimental procedure for the synthesis **1**, NMR spectra of ligands and complexes, catalysis optimization details, stoichiometric experiments, as well as X-ray data for **1**, **L^{Ph}**, **$[FeL^{Et}Cl_2]$, $[CoL^{Et}Cl_2]$, $[FeL^RBr_2]$** (R= Et, Cy)**, $[M(L^{Cy})_2Cl_2]$** (M=Fe, Co).

5. Acknowledgements

The authors thank Ecole Polytechnique, CNRS for financial support, Agence Nationale de la Recherche (ANR-21-CE07-0026) for funding the LYMACATO project, and RESOMAG platform for the access to NMR instruments. GDR Phosphore is also acknowledged for gathering the community of P-chemist in France.

6. References

1. (a) D. Wang; D. Astruc, The Golden Age of Transfer Hydrogenation. *Chem. Rev.* 2015, *115* (13), 6621-6686, https://doi.org/10.1021/acs.chemrev.5b00203; (b) B. Štefane; F. Požgan, Metal-Catalysed Transfer Hydrogenation of Ketones. In *Hydrogen Transfer Reactions: Reductions and Beyond*, Guillena, G.; Ramón, D. J., Eds. Springer International Publishing: Cham, 2016; pp 1-67; (c) E. Baráth. Hydrogen Transfer Reactions of Carbonyls, Alkynes, and Alkenes with Noble Metals in the Presence of Alcohols/Ethers and Amines as Hydrogen Donors *Catalysts* [Online], 2018, p. 671.
2. (a) T. Nidhi; B. Gongutri; P. Pitambar; R. Danaboyina, Recent Advances in Ru Catalyzed Transfer Hydrogenation and Its Future Perspectives. In *Ruthenium*, Hitoshi, I., Ed. IntechOpen: Rijeka, 2021; (b) M. Pilar Lamata; V. Passarelli; D. Carmona, Recent Advances in Iridium-Catalysed Transfer Hydrogenation Reactions. In *Iridium Catalysts for Organic Reactions*, Oro, L. A.; Claver, C., Eds. Springer International Publishing: Cham, 2021; pp 67-152.
3. D. Baidilov; D. Hayrapetyan; A. Y. Khalimon, Recent advances in homogeneous base-metal-catalyzed transfer hydrogenation reactions. *Tetrahedron* 2021, *98*, 132435, https://doi.org/https://doi.org/10.1016/j.tet.2021.132435.
4. D. Wei; C. Darcel, Iron Catalysis in Reduction and Hydrometalation Reactions. *Chem. Rev.* 2019, *119* (4), 2550-2610, https://doi.org/10.1021/acs.chemrev.8b00372.

5. F. Kallmeier; R. Kempe, Manganese Complexes for (De)Hydrogenation Catalysis: A Comparison to Cobalt and Iron Catalysts. *Angew. Chem. Int. Ed.* **2018,** *57* (1), 46-60, https://doi.org/https://doi.org/10.1002/anie.201709010.
6. V. Vermaak; H. C. M. Vosloo; A. J. Swarts, The development and application of homogeneous nickel catalysts for transfer hydrogenation and related reactions. *Coord. Chem. Rev.* **2024,** *507*, 215716, https://doi.org/https://doi.org/10.1016/j.ccr.2024.215716.
7. (a) K. Azouzi; D. A. Valyaev; S. Bastin; J.-B. Sortais, Manganese—New prominent actor in transfer hydrogenation catalysis. *Curr. Opin. Green Sustain. Chem.* **2021,** *31*, 100511, https://doi.org/https://doi.org/10.1016/j.cogsc.2021.100511; (b) Q. Liang; C. Zhang; F. Wang; Z. Luo; W. Yang; G. Zhang; D. Ding; G. Zhang, Triazole backbone ligand in an unprecedented efficient manganese catalyst for use in transfer hydrogenation. *Sci. China Chem.* **2023,** *66* (7), 2028-2036, https://doi.org/10.1007/s11426-022-1576-5.
8. R. T. Kumah; F. K. Migwi; M. Schmitz; W. R. Thiel; S. O. Ojwach, Novel Metallomacrocyclic Carboxamide Mn(II) Complexes as Efficient Catalysts for the Transfer Hydrogenation of Ketones. *ChemCatChem* **2023,** *15* (23), e202300971, https://doi.org/https://doi.org/10.1002/cctc.202300971.
9. G. Zhang; S. K. Hanson, Cobalt-catalyzed transfer hydrogenation of C=O and C=N bonds. *Chem. Commun.* **2013,** *49* (86), 10151-10153, https://doi.org/10.1039/C3CC45900D.
10. S. Huo; H. Chen; W. Zuo, A Cobalt(II) Complex Bearing the Amine(imine)diphosphine PN(H)NP Ligand for Asymmetric Transfer Hydrogenation of Ketones. *Eur. J. Inorg. Chem.* **2021,** *2021* (1), 37-42, https://doi.org/https://doi.org/10.1002/ejic.202000826.
11. (a) B.-L. Jiang; S.-S. Ma; M.-L. Wang; D.-S. Liu; B.-H. Xu; S.-J. Zhang, Cobalt-Catalyzed Chemoselective Transfer Hydrogenation of C=C and C=O Bonds with Alkanols. *ChemCatChem* **2019,** *11* (6), 1701-1706, https://doi.org/https://doi.org/10.1002/cctc.201900010; (b) S. Abubakar; M. D. Bala, Transfer Hydrogenation of Ketones Catalyzed by Symmetric Imino-N-heterocyclic Carbene Co(III) Complexes. *ACS Omega* **2020,** *5* (6), 2670-2679, https://doi.org/10.1021/acsomega.9b03181; (c) J. J. Ibrahim; C. B. Reddy; X. Fang; Y. Yang, Efficient Transfer Hydrogenation of Ketones Catalyzed by a Phosphine-Free Cobalt-NHC Complex. *Eur. J. Org. Chem.* **2020,** *2020* (28), 4429-4432, https://doi.org/https://doi.org/10.1002/ejoc.202000654; (d) S. Yadav; D. Prabha; D. Ahluwalia; A. Bag; R. Gupta, Cobalt Complexes as Efficient Cooperative Catalysts for Transfer Hydrogenation. *Eur. J. Org. Chem.* **2022,** *2022* (46), e202201059, https://doi.org/https://doi.org/10.1002/ejoc.202201059; (e) S.-H. Ruan; Z.-W. Fan; W.-J. Zhang; H. Xu; D.-L. An; Z.-B. Wei; R.-M. Yuan; J.-X. Gao; Y.-Y. Li, Asymmetric transfer hydrogenation of ketones catalyzed by chiral macrocyclic cobalt(II) complexes. *J. Catal.* **2023,** *418*, 100-109, https://doi.org/https://doi.org/10.1016/j.jcat.2023.01.008; (f) R. Yu; X. Zhang; F. Hao; Z. Jin; G. Liu; G. Dai; J. Wu, Cobalt-Promoted Transfer Hydrogenation of Azaaryl Ketones by Using Formate as the Hydrogen Source. *Eur. J. Org. Chem.* **2023,** *26* (15), e202300071, https://doi.org/https://doi.org/10.1002/ejoc.202300071.
12. (a) S. E. García-Garrido; A. Presa Soto; J. García-Álvarez, Chapter Three - Iminophosphoranes (R3PNR'): From terminal to multidentate ligands in organometallic chemistry. In *Advances in Organometallic Chemistry*, Pérez, P. J., Ed. Academic Press: 2022; Vol. 77, pp 105-168; (b) T. Tannoux; A. Auffrant, Complexes featuring tridentate iminophosphorane ligands: Synthesis, reactivity, and catalysis. *Coord. Chem. Rev.* **2023,** *474*, 214845, https://doi.org/https://doi.org/10.1016/j.ccr.2022.214845.
13. (a) V. Cadierno; P. Crochet; J. Diez; J. Garcia-Alvarez; S. E. Garcia-Garrido; S. Garcia-Granda; J. Gimeno; M. A. Rodriguez, Synthesis, reactivity and catalytic activity in transfer hydrogenation of ketones of ruthenium(II) and ruthenium(IV) complexes containing the novel N-thiophosphorylated iminophosphorane-phosphine ligands $Ph_2PCH_2P\{=NP(=S)(OR)_2\}Ph_2$ (R = Et, Ph). *Dalton Trans.* **2003,** (16), 3240-3249, https://doi.org/10.1039/b305520e; (b) V. Cadierno; P. Crochet; J. Diez; J. Garcia-Alvarez; S. E. Garcia-Garrido; J. Gimeno; S. Garcia-Granda; M. A. Rodriguez, Ruthenium(II) and ruthenium(IV) complexes containing kappa(1)-P-, kappa(2)-P,O-, and kappa(3)-P,N,O-iminophosphorane-phosphine ligands $Ph_2PCH_2P\{=NP(=O)(OR)_2\}Ph_2$ (R = Et, Ph): Synthesis, reactivity, theoretical studies, and catalytic activity in transfer hydrogenation of cyclohexanone. *Inorg. Chem.* **2003,** *42* (10), 3293-3307, https://doi.org/10.1021/ic020702k.

14. (a) A. Picot; H. Dyer; A. Buchard; A. Auffrant; L. Vendier; P. Le Floch; S. Sabo-Etienne, Interplay between Hydrido/Dihydrogen and Amine/Amido Ligands in Ruthenium-Catalyzed Transfer Hydrogenation of Ketones. *Inorg. Chem.* **2010,** *49* (4), 1310-1312, https://doi.org/10.1021/ic902339j; (b) H. Dyer; A. Picot; L. Vendier; A. Auffrant; P. Le Floch; S. Sabo-Etienne, Tridentate and Tetradentate Iminophosphorane-Based Ruthenium Complexes in Catalytic Transfer Hydrogenation of Ketones. *Organometallics* **2011,** *30* (6), 1478-1486, https://doi.org/10.1021/om101058m.
15. A. Buchard; E. Payet; A. Auffrant; X. Le Goff; P. Le Floch, Iminophosphorane-based P(2)N(2) rhodium complexes: synthesis, reactivity, and application in catalysed transfer hydrogenation of polar bonds. *New J. Chem.* **2010,** *34* (12), 2943-2949, https://doi.org/10.1039/c0nj00299b.
16. A. Buchard; H. Heuclin; A. Auffrant; X. F. Le Goff; P. Le Floch, Coordination of tetradentate X(2)N(2) (X = P, S, O) ligands to iron(II) metal center and catalytic application in the transfer hydrogenation of ketones. *Dalton Trans.* **2009,** (9), 1659-1667, https://doi.org/10.1039/b816439h.
17. (a) Z. H. Mou; B. Liu; X. L. Liu; H. Y. Xie; W. F. Rong; L. Li; S. H. Li; D. M. Cui, Efficient and Heteroselective Heteroscorpionate Rare-Earth-Metal Zwitterionic Initiators for ROP of rac-Lactide: Role of sigma-Ligand. *Macromolecules* **2014,** *47* (7), 2233-2241, https://doi.org/10.1021/ma500209t; (b) Z. H. Mou; H. Y. Xie; M. Y. Wang; N. Liu; C. G. Yao; L. Li; J. Y. Liu; S. H. Li; D. M. Cui, Mononuclear Heteroscorpionate Zwitterionic Zinc Terminal Hydride: Synthesis, Reactivity, and Catalysis for Hydrosilylation of Aldehydes. *Organometallics* **2015,** *34* (16), 3944-3949, https://doi.org/10.1021/acs.organomet.5b00413; (c) N. Liu; D. D. Liu; B. Liu; H. Zhang; D. M. Cui, Stereoselective polymerization of rac-lactide catalyzed by zwitterionic calcium complexes. *Polym. Chem.* **2021,** *12* (10), 1518-1525, https://doi.org/10.1039/d0py01397h.
18. O. Kühl, *Phosphorus-31 NMR Spectroscopy: A Concise Introduction for the Synthetic Organic and Organometallic Chemist*. 2009; p 1-131.
19. T. Cheisson; A. Auffrant; G. Nocton, eta(5)-eta(1) Switch in Divalent Phosphaytterbocene Complexes with Neutral Iminophosphoranyl Pincer Ligands: Solid-State Structures and Solution NMR (1)J(Yb-P) Coupling Constants. *Organometallics* **2015,** *34* (22), 5470-5478, https://doi.org/10.1021/acs.organomet.5b00814.
20. S. Eguchi; K. Yamashita; Y. Matsushita; A. Kakehi, Facile Synthesis of 1,4-Benzodiazepin-5-one Derivatives via Intramolecular Aza-Wittig Reaction. Application to an Efficient Synthesis of O-Benzyl DC-81. *J. Org. Chem.* **1995,** *60* (13), 4006-4012, https://doi.org/10.1021/jo00118a016.
21. (a) D. J. Evans; M. S. Hill; P. B. Hitchcock, Tuning low-coordinate metal environments: high spin d5–d7 complexes supported by bis(phosphinimino)methyl ligation. *Dalton Trans.* **2003,** (4), 570-574, https://doi.org/10.1039/B210467A; (b) M. S. Hill; P. B. Hitchcock, Three-coordinate bis(phosphinimino)methanide derivatives of 'open shell' [M(II)] (M=Mn, Fe, Co) transition metals. *J. Organomet. Chem.* **2004,** *689* (20), 3163-3167, https://doi.org/https://doi.org/10.1016/j.jorganchem.2004.06.050.
22. E. M. Schubert, Utilizing the Evans method with a superconducting NMR spectrometer in the undergraduate laboratory. *J. Chem. Educ.* **1992,** *69* (1), 62, https://doi.org/10.1021/ed069p62.1.
23. A. W. Addison; T. N. Rao; J. Reedijk; J. van Rijn; G. C. Verschoor, Synthesis, structure, and spectroscopic properties of copper(II) compounds containing nitrogen–sulphur donor ligands; the crystal and molecular structure of aqua[1,7-bis(N-methylbenzimidazol-2′-yl)-2,6-dithiaheptane]copper(II) perchlorate. *J. Chem. Soc. Dalton Trans.* **1984,** (7), 1349-1356, https://doi.org/10.1039/DT9840001349.
24. T. Tannoux; L. Mazaud; T. Cheisson; N. Casaretto; A. Auffrant, FeII complexes supported by an iminophosphorane ligand: synthesis and reactivity. *Dalton Trans.* **2023,** *52* (34), 12010-12019, https://doi.org/10.1039/D3DT00950E.
25. P. Schiltz; N. Casaretto; A. Auffrant; C. Gosmini, Cobalt Complexes Supported by Phosphinoquinoline Ligands for the Catalyzed Hydrosilylation of Carbonyl Compounds. *Chem. Eur. J.* **2022,** *28* (32), https://doi.org/10.1002/chem.202200437.
26. R. Cariou; F. Dahcheh; T. W. Graham; D. W. Stephan, Mononuclear and dinuclear palladium and nickel complexes of phosphinimine-based tridentate ligands. *Dalton Trans.* **2011,** *40* (18), 4918-4925, https://doi.org/10.1039/C1DT10131E.

27. For a comparable blank experiment see: C. Zhang; B. Hu; D. Chen; H. Xia, Manganese(I)-Catalyzed Transfer Hydrogenation and Acceptorless Dehydrogenative Condensation: Promotional Influence of the Uncoordinated N-Heterocycle. *Organometallics* **2019,** *38* (16), 3218-3226, https://doi.org/10.1021/acs.organomet.9b00475.
28. S. E. Clapham; A. Hadzovic; R. H. Morris, Mechanisms of the H2-hydrogenation and transfer hydrogenation of polar bonds catalyzed by ruthenium hydride complexes. *Coord. Chem. Rev.* **2004,** *248* (21), 2201-2237, https://doi.org/https://doi.org/10.1016/j.ccr.2004.04.007.
29. G. Zhang; B. L. Scott; S. K. Hanson, Mild and Homogeneous Cobalt-Catalyzed Hydrogenation of C=C, C=O, and C=N Bonds. *Angew. Chem. Int. Ed.* **2012,** *51* (48), 12102-12106, https://doi.org/https://doi.org/10.1002/anie.201206051.
30. G. Sheldrick, SHELXT - Integrated space-group and crystal-structure determination. *Acta Crystallogr., Sect. A* **2015,** *71* (1), 3-8, https://doi.org/doi:10.1107/S2053273314026370.
31. O. V. Dolomanov; L. J. Bourhis; R. J. Gildea; J. A. K. Howard; H. Puschmann, OLEX2: a complete structure solution, refinement and analysis program. *J. Appl. Crystallogr.* **2009,** *42* (2), 339-341, https://doi.org/doi:10.1107/S0021889808042726.
32. G. Sheldrick, Crystal structure refinement with SHELXL. *Acta Crystallogr., Sect. C* **2015,** *71* (1), 3-8, https://doi.org/doi:10.1107/S2053229614024218.
33. L. J. Farrugia *ORTEP-3 program*, Department of Chemistry, University of Glasgow: 2001.